Journal of Applied Analysis and Computation
Volume 16, Number 6, December 2026, 3201–3231
Website:http://www.jaac-online.com
DOI:10.11948/20260032

BIFURCATION ANALYSIS OF A DELAYED PREDATOR-PREY MODEL WITH GLOBAL WARMING, WIND FLOW, HUNTING COOPERATION AND FEAR EFFECT

Miao Peng[1,†], Rui Zhu[1] and Zhengdi Zhang[1]

Abstract The impacts of abiotic factors on species are of great research significance. With the intensification of global warming, the interactions among species have become increasing complex. Meanwhile, species activities can exacerbate global warming, which in turn exerts multifaceted influences on the environmental carrying capacity of species, the predation processes, etc. Wind flow is an omnipresent component of the natural environment, and existing studies have indicated that wind speed exerts a notable influence on the predation efficiency of predators for their prey. Although abiotic factors are ubiquitous in nature, studies investigating their impacts on species interactions remain relatively scarce. In this paper, we propose a delayed predator-prey model that incorporates global warming and wind flow, as well as other factors including hunting cooperation and fear effect. First, we discuss the non-delayed model and prove the positivity and boundedness of the solutions. Then, the analysis of the related characteristic equations enables us to examine the existence and local stability of four equilibria. We also discuss the existence of bifurcations near different equilibria. For the model with time delay, the local stability of the positive equilibrium and the existence of Hopf bifurcation are addressed in our discussion. Furthermore, we analyze the direction of Hopf bifurcation and the stability of the periodic solutions by the center manifold theorem and normal form method. Finally, some numerical simulations are given to support our findings.

Keywords Predator-prey model, stability analysis, Hopf bifurcation, numerical simulation.

MSC(2010) 34C23, 34D20, 34K18, 92D25.

1. Introduction

Interactions between predators and prey are universally existent in nature. Mathematical modeling of such interaction has become a crucial focus in the fields of ecology and biology. The classical predator-prey model was initially introduced by Lotka and Volterra [19, 45]. To enrich the Lotka-Volterra model, many factors have been incorporated such as functional response, harvesting, refuge, fear effect, etc. [26, 27, 29, 33].

In a predator-prey system, the functional response is defined as the per capita feeding rate of predators on their prey and serves as a crucial driver of population dynamics. Several scholars have conducted research using various types of functional responses, such as Holling types I-IV [9, 26, 33, 48] where Holling type I and type II functional responses are often used to analyze invertebrates, Holling type III functional responses are commonly applied to the analysis

[†]The corresponding author.
[1]School of Mathematical Sciences, Jiangsu University, Zhenjiang 212013, Jiangsu, China
Email: pengmiao@ujs.edu.cn(M. Peng), 13270367138@163.com(R. Zhu),
dyzhang@ujs.edu.cn(Z. Zhang)

of vertebrates, while Holling type IV functional responses are suitable for situations where prey density is excessively high, which in turn disrupts the predation process. The Lotka-Volterra model assumes that the per capita growth rate of predators depends on prey density. For instance, Holling type II functional response $p(x) = \frac{ex}{x+m}$ is widely employed in ecological models, which is only dependent on prey populations. Here, x denotes the prey density, e represents the predation efficiency, and m is the half-saturation constant. However, real-world scenarios are considerably more complex. The ratio-dependent theory [1] posits that the per capita growth rate of predators is related to the ratio of prey density to predator density. Replacing x with $\frac{x}{y}$, the ratio-dependent Holling type II functional response $p(x, y) = \frac{ex}{x+my}$ is obtained. Many scholars have incorporated ratio-dependent functional responses into model construction to investigate stability and bifurcation phenomena [34, 47].

Hunting cooperation means predators capture prey more effectively through cooperation, which can increase hunting success rates [5, 23, 37, 44]. This behavior is relatively common in social hunting species. The impacts of predators can be direct or indirect. Predators can exert direct impacts on prey populations through hunting, and can also cause indirect influence by inducing fear in prey [24]. Fear effect refers to behavioral and stress-related physiological changes in prey populations when predators are present. When prey perceive the presence of nearby predators, they may adopt a series of anti-predator behaviors, such as altering their activity patterns, shortening the time spent foraging, or moving to habitats with lower suitability to avoid predation, etc. [4, 21, 36, 46]. This fear can obviously affect the reproduction of the prey population.

With the deepening of research on population dynamics, abiotic factors such as global warming have been incorporated into the modeling. Global warming refers to a climatic phenomenon where greenhouse gas emissions caused by human activities lead to a continuous rise in Earth's average temperature [12]. This phenomenon has numerous impacts on the relationships between species. MacLean and Wilson [20] derived empirical evidence indicating that under the impact of climate change, the probability of extinction for all species is 14%. Numerous studies have indicated that global warming has impacts on species' birth rates, food availability, carrying capacity or fatality rate. In [40], an eco-epidemiological model was used to study the complex dynamics of predator-prey system, which considers the impact of global warming on the growth of both prey and predators. In [41], the researchers argued that the intensification of global warming would lead to a decrease in the densities of prey and predator species by analyzing a fractional-order model. Jawad et al. [13] established an ecological model to investigate the impact of global warming on the mortality rates of bees and plants. The researchers studied an ecological model in [37] which clarifies the predator-prey relationship and how global warming affects the carrying capacity of the prey. A three-dimensional model considering global warming, hunting cooperation, and fear effect was proposed in [39] as follows:

$$\begin{cases} \dfrac{dx}{dt} = x\left(\dfrac{r_1}{1+ay}\left(1-\dfrac{x}{k_1-\xi_1 g}\right)-\dfrac{(\alpha+\beta y+bg)y}{h(\alpha+\beta y+bg)x+1}\right), \\ \dfrac{dy}{dt} = y\left(r_2\left(1-\dfrac{y}{k_2-\xi_2 g}\right)+\dfrac{e\,(\alpha+\beta y+bg)x}{h(\alpha+\beta y+bg)x+1}-\mu_1\right), \\ \dfrac{dg}{dt} = a_1+a_2x+a_3y-\mu_2 g, \end{cases} \tag{1.1}$$

in which x stands for the prey density, y represents the predator density and g is global warming at time t. r_1 and r_2 are the logistic growth rate of prey and predator, respectively; a is the fear effect, k_1, k_2 represent the carrying capacity of prey and predator, respectively; ξ_1 and ξ_2 denote

the global warming effect on carrying capacity of prey and predator, respectively; α represents the encounter rate and β denotes the intensity of predators' cooperative hunting behavior, while h is handling time; b represents the rate at which global warming influences the predation process and μ_1 stands for the mortality rate of predators; a_1 is the density of global warming; a_2 and a_3 are the contribution to global warming by prey and predator, respectively; μ_2 is the global warming decay rate. They visualized dynamic changes using bifurcation diagrams and observed that the system undergoes different bifurcations as the value of ξ_2, which associated with global warming, increases. Through these analyses, we find that global warming exerts multifaceted impacts on ecosystems, and incorporating it into model construction allows for the observation of more complex dynamical phenomena.

In addition, wind is another persistent abiotic factor that cannot be ignored, as it can change how predators conduct their predation based on wind speed. Examples can be cited in different environments. Wind can influence the ability of species to perceive danger signals from predators [8]. Klimczuk et al. [14] found that reed warblers may exhibit more cautious behavior to avoid being blown off their nests or exposed to predators, during windy weather. To a certain extent, wind may affect the capture rate of predators. Cherry and Barton [3] showed that wind reduces animals' ability to detect other animals. For predators, this leads to an increase in the difficulty of detecting prey. Wind can reduce predator predation efficiency, which means that prey populations are supported with the help of wind [16,43]. Thirthar et al. [38,42] constructed predator-prey models incorporating wind effects and investigated various bifurcation phenomena. The researchers in [2] established a system considering wind and herd behavior to explore the impact of wind on the system and investigate various bifurcation phenomena of the system. Generally speaking, the impact of wind needs to be considered when conducting an ecosystem model.

In fact, all biological processes require time to complete. Therefore, it is necessary to consider time delays when modeling biological processes [18, 28]. Delay differential equations exhibit greater complexity. Time delays can alter the stability of the equilibria and cause fluctuations in population sizes. Various types of time delays have been taken into account by some researchers such as gestation delay [15,28], feedback delay [11,22], or different types of delays together [17,25]. They conducted research on the stability of equilibria, studied the presence of chaos, and explored bifurcation phenomena such as Hopf bifurcation, sliding bifurcation, etc.

For the ratio-dependent functional response $p(x, y) = \frac{ex}{x+my}$, we incorporate the following factors:

- Consider the impact of global warming g on the predation process.
- Incorporate the impacts of cooperative hunting on predation efficiency.
- Consider the impact of wind speed on the system. Use $1 + w$ to characterize the effect of wind on the prey's handling time, where w denotes the wind speed. The corresponding biological implications are presented by:
  - (i) Without the existence of wind flow, the predator's handling time for prey remains constant.
  - (ii) In windy conditions, we assume that the predator's handling time for prey increases linearly with wind speed.

The functional response becomes:

$$p(x, y, g) = \frac{e(1 + w)(\alpha + \beta y + bg)xy}{(1 + w)(\alpha + \beta y + bg)x + my}.$$

- Consider the fear response delay of prey.

Based on the work of [39] and the above analysis, we propose a mathematical model:

$$\begin{cases} \dfrac{dx}{dt} = x\left(\dfrac{r_1}{1+ky(t-\tau)}\left(1-\dfrac{x}{k_1-s_1g}\right)-\dfrac{(1+w)(\alpha+\beta y+dg)y}{(1+w)(\alpha+\beta y+dg)x+my}\right), \\ \dfrac{dy}{dt} = y\left(r_2\left(1-\dfrac{y}{k_2-s_2g}\right)+\dfrac{e\,(1+w)(\alpha+\beta y+dg)x}{(1+w)(\alpha+\beta y+dg)x+my}-d_1\right), \\ \dfrac{dg}{dt} = b_1+b_2x+b_3y-d_2g. \end{cases} \tag{1.2}$$

The initial conditions for system (1.2) meet $x(0) > 0$, $y(0) > 0$, $g(0) > 0$, with all parameters taking positive values. The biological descriptions of all parameters of system (1.2) are given in Table 1.

The structure of this paper proceeds as follows. In Section 2, we prove that the solutions of the model without time delay are positive and bounded, and derive the conditions for the existence and stability of four equilibria of the model. We also analyze the existence of bifurcations around different equilibria. Next, we discuss the local stability of the interior equilibrium of the delayed model and the existence of a Hopf bifurcation, followed by an exploration of its properties in Section 3. Numerical simulations are presented in Section 4 to support the theoretical results. Finally, we present a conclusion to summarize the paper.

Table 1. The biological descriptions of all parameters of system (1.2).

Parameter	Biological description	Value
τ	Fear response delay	
r_1	Birth rate of prey	0.7
r_2	Birth rate of predator	0.17
k	Fear effect	1
k_1	Carrying capacity of prey	10
k_2	Carrying capacity of predator	10
s_1	Global warming effect on carrying capacity of prey	0.8
s_2	Global warming effect on carrying capacity of predator	1.3
α	The encounter rate	0.4
β	Intensity of cooperative hunting among predators	0.1
m	Saturation constant of half capture	2
w	Wind flow	0.1
e	Predation efficiency	0.5
d	Global warming rate on predation process	0.1
d_1	Death rate of predator	0.2
b_1	Density of global warming	0.1
b_2	Prey's contribution to global warming	0.1
b_3	Predator's contribution to global warming	0.3
d_2	Decay rate of global warming	0.2

2. Dynamical analysis of the non-delayed model

Setting $\tau = 0$, we get the non-delayed model:

$$\begin{cases} \dfrac{dx}{dt} = x\left(\dfrac{r_1}{1+ky}\left(1-\dfrac{x}{k_1-s_1g}\right) - \dfrac{(1+w)(\alpha+\beta y+dg)y}{(1+w)(\alpha+\beta y+dg)x+my}\right) := x\,G_1(x,y,g), \\ \dfrac{dy}{dt} = y\left(r_2\left(1-\dfrac{y}{k_2-s_2g}\right) + \dfrac{e\,(1+w)(\alpha+\beta y+dg)x}{(1+w)(\alpha+\beta y+dg)x+my} - d_1\right) := y\,G_2(x,y,g), \\ \dfrac{dg}{dt} = b_1 + b_2x + b_3y - d_2g := G_3(x,y,g). \end{cases} \tag{2.1}$$

Next, we will explore the positivity and boundedness of the solutions of system (2.1). Following this, we discuss the stability of all the equilibriums and the bifurcations around them.

2.1. Positivity and boundedness of the solution

Positivity represents the survival of the population, while boundedness implies that growth is naturally constrained due to limited resources. So, it is of great importance to show the positivity and boundedness.

Theorem 2.1. *When $x(0) = x_0 > 0, y(0) = y_0 > 0, g(0) = g_0 > 0$, the solution of system (2.1) is positive.*

Proof. By examining the first two equations in system (2.1), we obtain

$$x(t) = x(0)\exp\left(\int_0^t G_1(x(s),y(s),g(s))\,ds\right) \geq 0,$$
$$y(t) = y(0)\exp\left(\int_0^t G_2(x(s),y(s),g(s))\,ds\right) \geq 0.$$

For g, we have

$$\frac{dg}{dt} + d_2g = b_1 + b_2x + b_3y.$$

Obviously, $x(t) > 0, y(t) > 0$, so $\frac{dg}{dt} + d_2g > 0$. Assuming $H(x(t), y(t)) = \frac{dg}{dt} + d_2g$, we can get

$$g(t) = e^{-d_2t}\int_0^t H(x(t),y(t))e^{d_2t}dt + g(0)e^{-d_2t} > 0.$$

This proves that the solution $(x(t), y(t), g(t))$ remains positive with the initial conditions. □

Then, we establish the uniform boundedness of all solutions to system (2.1) through the theorem below.

Theorem 2.2. *Under any conditions, every solution of system (2.1) exhibits uniform boundedness in $\mathbb{R}^3_+$.*

Proof. Let $N = x + y + g$. By calculating its derivative, we have

$$\frac{dN}{dt} = \frac{dx}{dt} + \frac{dy}{dt} + \frac{dg}{dt}.$$

According to system (2.1), we know

$$\frac{dN}{dt} \leq x\left(\frac{r_1}{1+k_1y}\left(1-\frac{x}{k_1-s_1g}\right)\right) + yr_2\left(1-\frac{y}{k_2-s_2g}\right) + b_1 + b_2x + b_3y - d_2g - d_1y.$$

Because of $r_1 > \frac{r_1}{1+k_1 y}$, we can get

$$\frac{dN}{dt} \leq r_1 x\left(1-\frac{x}{k_1}\right) + yr_2 + b_1 + b_2 x + b_3 y - d_2 g.$$

Then, we add cN on both sides of the above inequality, where $c \in \mathbb{R}_+$. We have

$$\frac{dN}{dt} + cN \leq r_1 x\left(1-\frac{x}{k_1}\right) + yr_2 + b_1 + b_2 x + b_3 y + c\left(c-d_2\right) g + cx + cy,$$
$$\frac{dN}{dt} + cN \leq \frac{(r_1+b_2+c)k_1}{2}\left(1-\frac{ck_1+b_2+c}{2r_1}\right) + (b_2+c)\left(1-\frac{ck_1+b_2+c}{2r_1}\right) := \varsigma.$$

Defining $\varsigma > 0$, we have

$$\frac{dN}{dt} + cN \leq \varsigma.$$

With the theory of differential inequality [10], there are

$$0 < N(x,y,g) \leq \frac{\varsigma}{c}\left(1-e^{-ct}\right) + N(x(0),y(0),g(0))e^{-ct}.$$

So we obtain $0 < N < \frac{\varsigma}{c}$ for $t \to \infty$. In conclusion, all the solutions of system (2.1) are bounded in the positive region

$$\bar{Z} = \left\{(x,y,g) \in \mathbb{R}^3_+ : N \leq \frac{\varsigma}{c}\right\}.$$

□

2.2. Equilibrium analysis

Obviously, system (2.1) possesses four non-negative equilibria.

(i) The extinction equilibrium:

$$E_1 = \left(0, 0, \frac{b_1}{d_2}\right).$$

(ii) The predator free equilibrium:

$$E_2 = \left(\frac{k_1 d_2 - s_1 b_1}{d_2 + b_2 s_1}, 0, \frac{b_1 + b_2 k_1}{b_2 s_1 + d_2}\right).$$

E_2 exists when $k_1 d_2 > s_1 b_1$.

(iii) The prey free equilibrium:

$$E_3 = \left(0, \frac{(r_2-d_1)(k_2-s_2 G_3)}{r_2}, \frac{r_2 b_1 + b_3 k_2 (r_2-d_1)}{r_2 d_2 + s_2 b_3 (r_2-d_1)}\right).$$

E_3 exists if $(r_2-d_1)(k_2-s_2G_3) > 0$ and $G_3 > 0$, where $G_3 = \frac{r_2 b_1 + b_3 k_2 (r_2-d_1)}{r_2 d_2 + s_2 b_3 (r_2-d_1)}$.

(iv) The interior equilibrium:

$$E_4 = (x^*, y^*, g^*).$$

Using the second and third equations of system (2.1), we can express x^* and g^* in terms of y. We have

$$x^* = \frac{d_2 g^* - b_3 y - b_1}{b_2} := M_1(y),$$

and g^* is the root of the cubic equation below:

$$h_1h_4(g^*)^3 + (h_2h_4 + h_1h_5)(g^*)^2 + (h_3h_4 + h_2h_5 - h_6)g^* + h_3h_5 - h_7 = 0,$$

where

$$\begin{aligned}
&h_1 = (1+w)dd_2, \quad h_2 = (1+w)[d_2(\alpha+\beta y) - d(b_3y + b_1)],\\
&h_3 = -(1+w)(\alpha+\beta y)(b_3y+b_1), \quad h_4 = -s_2(ey - d_1 + r_2y),\\
&h_5 = k_2(ey - d_1 + r_2y) - r_2y^2, \quad h_6 = b_2my(r_2s_2y - d_1s_2),\\
&h_7 = b_2my(r_2y^2 + d_1k_2 - r_2k_2y).
\end{aligned}$$

Since g^* can be expressed by y, we denote g^* by $M_2(y)$. By substituting x^* and g^* into the first equation of system (2.1), we obtain

$$M^*(y) = \frac{r_1}{1+ky}\left(1 - \frac{M_1(y)}{k_1 - s_1M_2(y)}\right) - \frac{(1+w)[\alpha+\beta y + dM_2(y)]y}{(1+w)[\alpha+\beta y + dM_2(y)]M_1(y) + my}.$$

Obviously,

$$\begin{aligned}
M^*(0) &= r_1\left(1 - \frac{M_1(0)}{k_1 - s_1M_2(0)}\right),\\
M^*(a) &= \frac{r_1}{1+ky}\left(1 - \frac{M_1(a)}{k_1 - s_1M_2(a)}\right) - \frac{(1+w)[\alpha+\beta a + dM_2(a)]a}{(1+w)[\alpha+\beta a + dM_2(a)]M_1(a) + ma},
\end{aligned}$$

where $a = \min\{k_1, k_2\}$.
By the intermediate value theorem, $M^*(a)$ possesses a positive root (denoted $y = y^*$) in the interval $(0, a)$ if $M^*(0) > 0, M^*(a) < 0$ or $M^*(0) < 0, M^*(a) > 0$ is satisfied.

2.3. Stability analysis

In this part, we explore the local stability of different equilibria, and the corresponding local stability analyses are as follows:

(i) The extinction equilibrium is $E_1 = \left(0, 0, \frac{b_1}{d_2}\right)$, and the Jacobian matrix at this point is

$$J_{E_1} = \begin{pmatrix} r_1 & 0 & 0\\ 0 & r_2 - d_1 & 0\\ b_2 & b_3 & -d_2 \end{pmatrix}.$$

The corresponding characteristic equation is $(\lambda - r_1)(\lambda - r_2 + d_1)(\lambda + d_2) = 0$. Obviously, $\lambda_1 = r_1 > 0$, $\lambda_2 = r_2 - d_1$, $\lambda_3 = -d_2 < 0$. Therefore E_1 is a saddle which is unstable.

(ii) The predator free equilibrium is $E_2 = \left(\frac{k_1d_2 - s_1b_1}{d_2 + b_2s_1}, 0, \frac{b_1 + b_2k_1}{b_2s_1 + d_2}\right)$. The corresponding Jacobian matrix is presented as

$$J_{E_2} = \begin{pmatrix} -r_1 & -1 & -r_1s_1\\ 0 & r_2 + e - d_1 & 0\\ b_2 & b_3 & -d_2 \end{pmatrix}.$$

The related characteristic equation at E_2 is

$$(\lambda - r_2 - e + d_1)(\lambda^2 + B_1\lambda + B_2) = 0,$$

where $B_1 = r_1 + d_2$, $B_2 = r_1(d_2 + s_1 b_2)$.
Let $\lambda_1 = r_2 + e - d_1$. If $r_2 + e > d_1$, λ_1 is positive and E_2 is unstable. If $r_2 + e < d_1$, λ_1 is negative and E_2 is stable.

(iii) The prey free equilibrium is $E_3 = \left(0, \frac{(r_2-d_1)(k_2-s_2G_3)}{r_2}, \frac{r_2b_1+b_3k_2(r_2-d_1)}{r_2d_2+s_2b_3(r_2-d_1)}\right)$. Jacobian matrix can be presented at this equilibrium as:

$$J_{E_3} = \begin{pmatrix} \frac{r_1}{(kY_3+1)} - \frac{(1+w)(\alpha+\beta Y_3+dG_3)}{m} & 0 & 0 \\ \frac{e(1+w)(\alpha+\beta Y_3+dG_3)}{m} & d_1 - r_2 & \frac{-(r_2-d_1)^2 s_2}{r_2} \\ b_2 & b_3 & -d_2 \end{pmatrix},$$

where $Y_3 = \frac{(r_2-d_1)(k_2-s_2G_3)}{r_2}$ and $G_3 = \frac{r_2b_1+b_3k_2(r_2-d_1)}{r_2d_2+s_2b_3(r_2-d_1)}$.
By simple computation, the corresponding characteristic equation is

$$\begin{aligned}&(\lambda - \frac{r_1}{(kY_3+1)} + \frac{(1+w)(\alpha+\beta Y_3+dG_3)}{m}) \\ &\times (\lambda^2 + (d_2 + r_2 - d_1)\lambda + r_2d_2 - d_1d_2 + \frac{(r_2-d_1)^2 s_2 b_3}{r_2}) = 0.\end{aligned}$$

The corresponding eigenvalues are $\lambda_1 = \frac{r_1}{(kY_3+1)} - \frac{(1+w)(\alpha+\beta Y_3+dG_3)}{m}$, $\lambda_{2,3} = \frac{-B_3 \pm \sqrt{B_3^2 - 4B_4}}{2}$, where $B_3 = d_2 + r_2 - d_1, B_4 = r_2d_2 - d_1d_2 + \frac{(r_2-d_1)^2 s_2 b_3}{r_2}$. If $d_2 + r_2 < d_1$, we have $B_3 < 0$, which means E_3 is unstable. If $d_2 + r_2 > d_1$, we can get $B_3 > 0$. Therefore, E_3 exhibits local asymptotic stability under the condition that $\frac{r_1}{(kY_3+1)} < \frac{(1+w)(\alpha+\beta Y_3+dG_3)}{m}$.

(iv) The interior equilibrium is $E_4 = (x^*, y^*, g^*)$. For this equilibrium, the Jacobian matrix is defined as:

$$J_{E_4} = \begin{pmatrix} t_{11}^* & t_{12}^* & t_{13}^* \\ t_{21}^* & t_{22}^* & t_{23}^* \\ t_{31}^* & t_{32}^* & t_{33}^* \end{pmatrix}.$$

where

$$\begin{aligned}
t_{11}^* &= \frac{r_1}{1+ky^*}\left(1 - \frac{2x^*}{k_1 - s_1g^*}\right) - \frac{my^{*2}(1+w)(\alpha+\beta y^*+dg^*)}{[(1+w)(\alpha+\beta y^*+dg^*)x^* + my^*]^2}, \\
t_{12}^* &= \frac{-kr_1x^*}{(1+ky^*)^2}\left(1 - \frac{x^*}{k_1 - s_1g^*}\right) - \frac{x^*(1+w)(\alpha+2\beta y^*+dg^*)}{(1+w)(\alpha+\beta y^*+dg^*)x^* + my^*} \\
&\quad + \frac{x^*y^*(1+w)(\alpha+\beta y^*+dg^*)[(1+w)\beta x^* + m]}{[(1+w)(\alpha+\beta y^*+dg^*)x^* + my^*]^2}, \\
t_{13}^* &= -\frac{s_1x^{*2}}{(k_1 - s_1g^*)^2} \cdot \frac{r_1}{1+ky^*} - \frac{(1+w)dmy^{*2}x^*}{[(1+w)(\alpha+\beta y^*+dg^*)x^* + my^*]^2},
\end{aligned}$$

$$
\begin{aligned}
t_{21}^* &= \frac{e(1+w)(\alpha+\beta y^*+dg^*)my^{*2}}{[(1+w)(\alpha+\beta y^*+dg^*)x^*+my^*]^2},\\
t_{22}^* &= r_2\left(1-\frac{2y^*}{k_2-s_2g^*}\right)+\frac{ex^*(1+w)(\alpha+2\beta y^*+dg^*)}{(1+w)(\alpha+\beta y^*+dg^*)x^*+my^*}\\
&\quad -\frac{ex^*y^*(1+w)(\alpha+\beta y^*+dg^*)[(1+w)\beta x^*+m]}{[(1+w)(\alpha+\beta y^*+dg^*)x^*+my^*]^2}-d_1,\\
t_{23}^* &= \frac{-r_2s_2y^{*2}}{(k_2-s_2g^*)^2}+\frac{e(1+w)dmx^*y^{*2}}{[(1+w)(\alpha+\beta y^*+dg^*)x^*+my^*]^2},\\
t_{31}^* &= b_2,\quad t_{32}^*=b_3,\quad t_{33}^*=-d_2.
\end{aligned}
$$

The corresponding characteristic equation is

$$\lambda^3+c_1\lambda^2+c_2\lambda+c_3=0, \tag{2.2}$$

with

$$
\begin{aligned}
c_1 &= -(t_{11}^*+t_{22}^*+t_{33}^*),\\
c_2 &= t_{11}^*t_{22}^*-t_{12}^*t_{21}^*+t_{22}^*t_{33}^*-t_{23}^*t_{32}^*+t_{11}^*t_{33}^*-t_{13}^*t_{31}^*,\\
c_3 &= -(t_{11}^*t_{22}^*t_{33}^*-t_{11}^*t_{23}^*t_{32}^*-t_{12}^*t_{21}^*t_{33}^*+t_{12}^*t_{23}^*t_{31}^*+t_{13}^*t_{21}^*t_{32}^*-t_{13}^*t_{22}^*t_{31}^*),
\end{aligned}
$$

and λ is the eigenvalue. According to the Routh-Hurwitz criterion, the equilibrium will be locally asymptotically stable when the conditions $c_1>0$, $c_3>0$, and $c_1c_2>c_3$ are meet.

2.4. Transcritical bifurcation

Theorem 2.3. *The extinction equilibrium E_1 undergoes a transcritical bifurcation around $d_1=d_{1t}=r_2$.*

Proof. If $d_1=d_{1t}$ is chosen as the bifurcation parameter, the Jacobian matrix associated with E_1 will turn into

$$(J_{E_1})|_{d_{1t}}=\begin{pmatrix} r_1 & 0 & 0\\ 0 & 0 & 0\\ b_2 & b_3 & -d_2\end{pmatrix}.$$

It is obvious that the system possesses a zero eigenvalue. The eigenvectors associated with this zero eigenvalue of $(J_{E_1})|_{d_{1t}}$ and its transpose $(J_{E_1})^T\big|_{d_{1t}}$ are presented by $V=\begin{pmatrix}0\\ d_2\\ b_3\end{pmatrix}$ and $W=\begin{pmatrix}0\\ 1\\ 0\end{pmatrix}$ respectively. Let $F(x,y,g)=(\frac{dx}{dt},\frac{dy}{dt},\frac{dg}{dt})^T=(y_1,y_2,y_3)^T$, through computation we

have

$$F_{d_1}(E_1;d_{1t}) = \begin{pmatrix} \dfrac{\partial y_1}{\partial d_1} \\ \dfrac{\partial y_2}{\partial d_1} \\ \dfrac{\partial y_3}{\partial d_1} \end{pmatrix}_{(E_1;d_{1t})} = \begin{pmatrix} 0 \\ 0 \\ 0 \end{pmatrix},$$

$$DF_{d_1}(E_1;d_{1t})V = \begin{pmatrix} \dfrac{\partial y_{1d}}{\partial x} & \dfrac{\partial y_{1d}}{\partial y} & \dfrac{\partial y_{1d}}{\partial g} \\ \dfrac{\partial y_{2d}}{\partial x} & \dfrac{\partial y_{2d}}{\partial y} & \dfrac{\partial y_{2d}}{\partial g} \\ \dfrac{\partial y_{3d}}{\partial x} & \dfrac{\partial y_{3d}}{\partial y} & \dfrac{\partial y_{3d}}{\partial g} \end{pmatrix}_{(E_1;d_{1t})} \qquad V = \begin{pmatrix} 0 \\ -d_2 \\ 0 \end{pmatrix},$$

$$D^2F(E_1;d_{1t})(V,V) = \begin{pmatrix} 0 \\ \dfrac{-2r_2d_2^3}{k_2d_2 - s_2b_1} \\ 0 \end{pmatrix}.$$

Also

$$W^T[DF_{d_1}(E_1;d_{1t})V] = -d_2 \neq 0,$$
$$W^T[D^2F(E_1;d_{1t})(V,V)] = \frac{-2r_2d_2^3}{k_2d_2 - s_2b_1} \neq 0.$$

Utilizing the Sotomayor's Theorem [30], we can prove that system (2.1) experiences a transcritical bifurcation at $d_1 = d_{1t}$. □

2.5. Hopf bifurcation

Theorem 2.4. *There exists a critical value s_2^* of the effect of global warming on carrying capacity of predator s_2 if*

(i) $c_i(s_2^*) > 0$, $i = 1, 2$,

(ii) $c_3(s_2^*) - c_1(s_2^*)c_2(s_2^*) = 0$,

(iii) $\left(c_2\frac{\mathrm{d}c_1}{\mathrm{d}s_2} + c_1\frac{\mathrm{d}c_2}{\mathrm{d}s_2} - \frac{\mathrm{d}c_3}{\mathrm{d}s_2}\right)\Big|_{s_2=s_2^*} \neq 0$,

are satisfied. Then the positive equilibrium E_4 exhibits local asymptotic stability if $s_2 > s_2^*$, while it is unstable if $s_2 < s_2^*$. Moreover, a Hopf bifurcation occurs at E_4 if $s_2 = s_2^*$.

Proof. The value of the bifurcation parameter can be found if we set $c_3(s_2^*) - c_1(s_2^*)c_2(s_2^*) = 0$ in Eq. (2.2). Let $s_2 = s_2^*$, Eq. (2.2) can be rewritten as

$$(\lambda + c_1)(\lambda^2 + c_2) = 0. \tag{2.3}$$

Obviously, Eq. (2.3) possesses a real root $\lambda_1 = -c_1$ and a pair of conjugate virtual roots $\lambda_{2,3} = \pm i\sqrt{c_2}$. In a neighborhood of s_2^*, the roots can be presented by $\lambda_1 = -c_1, \lambda_{2,3} = \delta_1(s_2) \pm i\delta_2(s_2)$. When $s_2 = s_2^*$, the positive equilibrium E_4 has a pair of conjugate pure imaginary roots.

Using the method presented in [31], we differentiate both sides of Eq. (2.2) regarding s_2.

$$\frac{\mathrm{d}\lambda}{\mathrm{d}s_2} = -\frac{\frac{\mathrm{d}c_1(s_2)}{\mathrm{d}s_2}\lambda^2 + \frac{\mathrm{d}c_2(s_2)}{\mathrm{d}s_2}\lambda + \frac{\mathrm{d}c_3(s_2)}{\mathrm{d}s_2}}{3\lambda^2 + 2c_1\lambda + c_2},$$

$$\mathrm{Re}\left(\left.\frac{\mathrm{d}\lambda}{\mathrm{d}s_2}\right|_{\lambda=i\sqrt{c_2},s_2=s_2^*}\right) = \left.\frac{2c_2\left(c_2\frac{\mathrm{d}c_1(s_2)}{\mathrm{d}s_2} + c_1\frac{\mathrm{d}c_2(s_2)}{\mathrm{d}s_2} - \frac{\mathrm{d}c_3(s_2)}{\mathrm{d}s_2}\right)}{(\frac{\mathrm{d}c_3(s_2)}{\mathrm{d}s_2} - \frac{\mathrm{d}c_1(s_2)}{\mathrm{d}s_2}c_2)^2 + c_2(\frac{\mathrm{d}c_2(s_2)}{\mathrm{d}s_2})^2}\right|_{s_2=s_2^*}.$$

If a critical value s_2^* exists for s_2, satisfying

$$\left(c_2\frac{\mathrm{d}c_1}{\mathrm{d}s_2} + c_1\frac{\mathrm{d}c_2}{\mathrm{d}s_2} - \frac{\mathrm{d}c_3}{\mathrm{d}s_2}\right)\Big|_{s_2=s_2^*} \neq 0,$$

we obtain

$$\mathrm{Re}\left(\left.\frac{\mathrm{d}\lambda}{\mathrm{d}s_2}\right|_{\lambda=i\sqrt{c_2},s_2=s_2^*}\right) \neq 0,$$

which implies that the transversal condition is satisfied. Thus, the proof is concluded. □

3. Dynamical analysis of the delayed model

3.1. Local stability and Hopf bifurcation

In this section, we discuss the existence of the Hopf bifurcation of delayed system (1.2). To linearize the system (1.2) at equilibrium E_4, let $\bar{X}(t) = x(t) - x^*$, $\bar{Y}(t) = y(t) - y^*$, $\bar{G}(t) = g(t) - g^*$. Then we have

$$\begin{cases} \bar{X}(t) = a_{11}\bar{X}(t) + a_{12}\bar{Y}(t) + a_{13}\bar{G}(t) + b_{12}\bar{Y}(t-\tau), \\ \bar{Y}(t) = a_{21}\bar{X}(t) + a_{22}\bar{Y}(t) + a_{23}\bar{G}(t), \\ \bar{G}(t) = a_{31}\bar{X}(t) + a_{32}\bar{Y}(t) + a_{33}\bar{G}(t), \end{cases}$$

where

$$\begin{aligned}
a_{11} &= \frac{r_1}{1+ky^*}\left(1 - \frac{2x^*}{k_1 - s_1g^*}\right) - \frac{my^{*2}(1+w)(\alpha+\beta y^*+dg^*)}{[(1+w)(\alpha+\beta y^*+dg^*)x^* + my^*]^2}, \\
a_{12} &= -\frac{x^*(1+w)(\alpha+2\beta y^*+dg^*)}{(1+w)(\alpha+\beta y^*+dg^*)x^* + my^*} + \frac{x^*y^*(1+w)(\alpha+\beta y^*+dg^*)[(1+w)\beta x^*+m]}{[(1+w)(\alpha+\beta y^*+dg^*)x^* + my^*]^2}, \\
a_{13} &= -\frac{s_1x^{*2}}{(k_1 - s_1g^*)^2}\cdot\frac{r_1}{1+ky^*} - \frac{(1+w)dmy^{*2}x^*}{[(1+w)(\alpha+\beta y^*+dg^*)x^* + my^*]^2}, \\
a_{21} &= \frac{e(1+w)(\alpha+\beta y^*+dg^*)my^{*2}}{[(1+w)(\alpha+\beta y^*+dg^*)x^* + my^*]^2}, \\
a_{22} &= r_2\left(1 - \frac{2y^*}{k_2 - s_2g^*}\right) + \frac{ex^*(1+w)(\alpha+2\beta y^*+dg^*)}{(1+w)(\alpha+\beta y^*+dg^*)x^* + my^*} \\
&\quad - \frac{ex^*y^*(1+w)(\alpha+\beta y^*+dg^*)[(1+w)\beta x^*+m]}{[(1+w)(\alpha+\beta y^*+dg^*)x^* + my^*]^2} - d_1, \\
a_{23} &= \frac{-r_2s_2y^{*2}}{(k_2 - s_2g^*)^2} + \frac{e(1+w)dmx^*y^{*2}}{[(1+w)(\alpha+\beta y^*+dg^*)x^* + my^*]^2},
\end{aligned}$$

$$a_{31} = b_2, \quad a_{32} = b_3, \quad a_{33} = -d_2, \quad b_{12} = \frac{-kr_1x^*}{(1+ky^*)^2}\left(1 - \frac{x^*}{k_1 - s_1g^*}\right).$$

So, the characteristic equation is

$$\lambda^3 + p_2\lambda^2 + p_1\lambda + p_0 + (q_1\lambda + q_0)e^{-\lambda\tau} = 0, \tag{3.1}$$

where

$$\begin{aligned}
&p_0 = a_{13}a_{31}a_{22} + a_{32}a_{23}a_{11} + a_{33}a_{21}a_{12} - a_{11}a_{22}a_{33} - a_{21}a_{32}a_{13} - a_{31}a_{23}a_{12},\\
&p_1 = a_{11}a_{22} + (a_{11} + a_{12})a_{33} - a_{13}a_{31} - a_{32}a_{23} - a_{21}a_{12},\\
&p_2 = -(a_{11} + a_{22} + a_{33}), \quad q_0 = a_{33}a_{21}b_{12} - a_{31}a_{23}b_{12}, \quad q_1 = -a_{21}b_{12}.
\end{aligned}$$

In order to investigate the root distribution of Eq. (3.1), we continue the investigation by discussing the following cases:

Case 1. $\tau = 0$. In this case, Eq. (3.1) is reduced to

$$\lambda^3 + p_{12}\lambda^2 + p_{11}\lambda + p_{10} = 0, \tag{3.2}$$

where

$$p_{12} = p_2, \quad p_{11} = p_1 + q_1, \quad p_{10} = p_0 + q_0.$$

To ensure that all roots of Eq. (3.2) have negative real parts, we improve the condition $p_{12} > 0, p_{10} > 0, p_{12}p_{11} > p_{10}$, which are denoted by (H_1). Under condition (H_1), the equilibrium E_4 is locally asymptotically stable.

Case 2. $\tau \neq 0$. Let $i\omega(\omega > 0)$ be a root of Eq. (3.1). Under this assumption, we have

$$\begin{cases} q_1\omega\sin\omega\tau + q_0\cos\omega\tau = p_2\omega^2 - p_0, \\ q_1\omega\cos\omega\tau - q_0\sin\omega\tau = \omega^3 - p_1\omega. \end{cases} \tag{3.3}$$

If we square each side of Eq. (3.3) and add the two squared expressions, respectively, we have

$$\omega^6 + e_{12}\omega^4 + e_{11}\omega^2 + e_{10} = 0, \tag{3.4}$$

where

$$e_{12} = p_2^2 - 2p_1, \quad e_{11} = p_1^2 - 2p_0p_2 - q_1^2, \quad e_{10} = p_0^2 - q_0^2.$$

If we have $\omega^2 = z$, Eq. (3.4) becomes

$$z^3 + e_{12}z^2 + e_{11}z + e_{10} = 0. \tag{3.5}$$

Denote $U(z) = z^3 + e_{12}z^2 + e_{11}z + e_{10}$, then $U(0) = e_{10}$, $\lim\limits_{z\to+\infty} U(z) = +\infty$, $U'(z) = 3z^2 + 2e_{12}z + e_{11}$. Using the approach presented in [32], we discuss the roots of Eq. (3.5) and obtain the conditions below:

$$\begin{aligned}
&(H_2): \ e_{10} \geq 0, \ \Delta = e_{12}^2 - 3e_{11} \leq 0,\\
&(H_3): \ e_{10} \geq 0, \ \Delta = e_{12}^2 - 3e_{11} > 0, \ z^* = \frac{-e_{12} + \sqrt{\Delta}}{3} > 0, \ U(z^*) \leq 0,\\
&(H_4): \ e_{10} < 0.
\end{aligned}$$

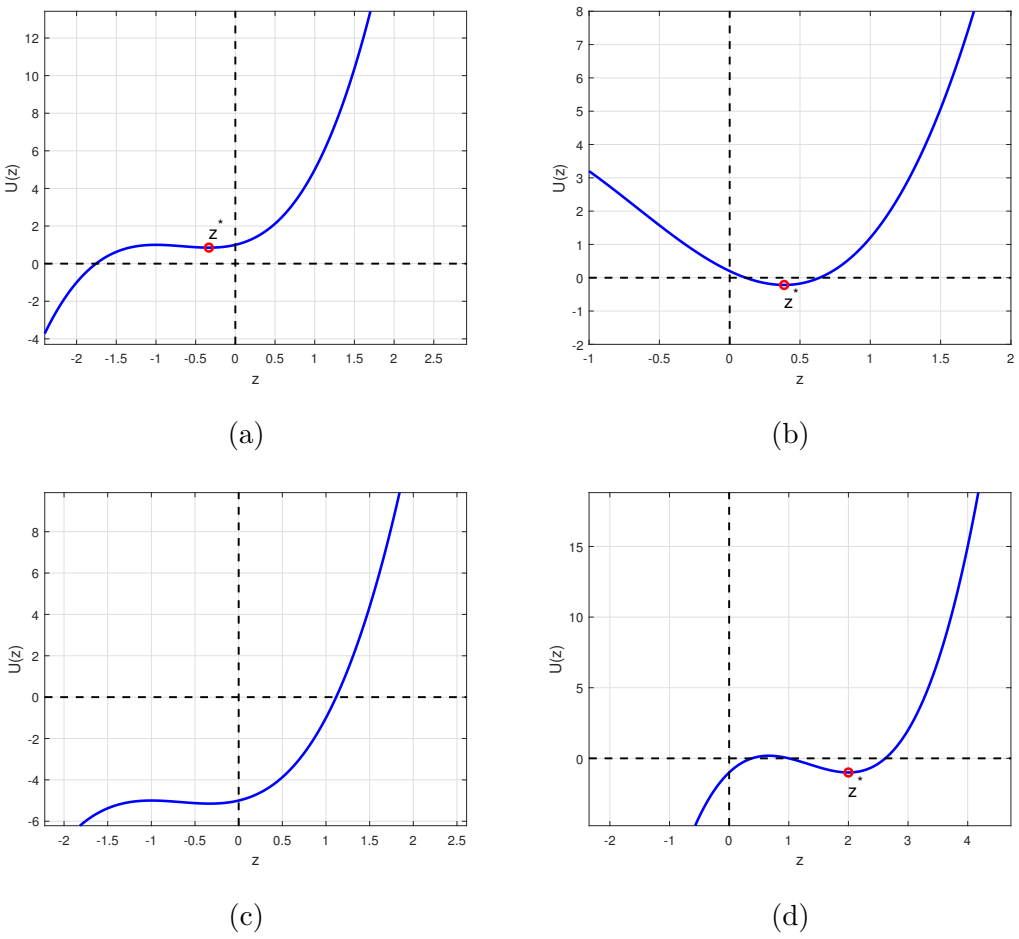

Figure 1. Analysis of the number of solutions to Eq. (3.5) where the blue curve represents the function $U(z)$ and the red circle denotes its local minimum point z^*. (a) Eq. (3.5) has none positive root under (H_2). (b) Eq. (3.5) has two positive roots under (H_3). (c) Eq. (3.5) has one positive root under (H_4). (d) Eq. (3.5) has three positive roots under (H_4).

We plot the graphs of $U(z)$ under the above conditions. There is no intersection between $U(z)$ and the positive half of the x-axis under the condition (H_2). In Figure 1(b), since $U(z^*) \leq 0$, Eq. (3.5) may have one or two positive solutions. From Figure 1(c) and (d), Eq. (3.5) has at least one positive solution if condition (H_3) holds.

From the above analysis, the following lemma is obtained.

Lemma 3.1. *For Eq.* (3.5),

(1) If the condition (H_2) *is satisfied, there are no positive roots in Eq.* (3.5).

(2) If the condition (H_3) *or the condition* (H_4) *holds, Eq.* (3.5) *possesses at least one positive root.*

Assume there exist three positive roots for Eq. (3.5), and let these roots be denoted as z_1, z_2 and z_3. So Eq. (3.4) possesses three positive roots $\omega_k = \sqrt{z_k}, k = 1, 2, 3$. Through Eq. (3.3), we

can express the critical time delay value as

$$\tau_k^{(j)} = \frac{1}{\omega_k} \arccos\left(\frac{A_{40}\omega_k^4 + A_{20}\omega_k^2 + A_{10}}{B_{20}\omega_k^2 + B_{10}}\right) + \frac{2\pi j}{\omega_k},\ k = 1,2,3;\ j = 0,1,2,\ldots, \tag{3.6}$$

where $A_{40} = q_1$, $A_{20} = p_2q_0 - p_1q_1$, $A_{10} = -p_0q_0$, $B_{20} = q_1^2$, $B_{10} = q_0^2$. Therefore, we regard $\lambda(\tau) = \varsigma(\tau) + i\omega(\tau)$ as a root of Eq. (3.1) with $\varsigma(\tau_k^{(j)}) = 0$, $\omega(\tau_k^{(j)}) = \omega_k$, and make $\tau_0 = \min\limits_{k\in\{1,2,3\}}\{\tau_k^{(j)}\}$, $\omega_0 = \omega_k$.

To ensure the transversality condition holds, we require $U'(\omega_0^2) \neq 0$, which is denoted by (H_5). We subsequently establish the following lemma:

Lemma 3.2. *If (H_5) holds, then $\left.\frac{\mathrm{dRe}(\lambda)}{\mathrm{d}\tau_0}\right|_{\lambda=i\omega_0} \neq 0$ is obtained.*

Proof. Taking derivative of Eq. (3.1) with regard to τ, we derive

$$\left(\frac{\mathrm{d}\lambda}{\mathrm{d}\tau}\right)^{-1} = -\frac{3\lambda^2 + 2p_2\lambda + p_1}{\lambda(\lambda^3 + p_2\lambda^2 + p_1\lambda + p_0)} + \frac{q_1}{\lambda(q_1\lambda + q_0)} - \frac{\tau}{\lambda}. \tag{3.7}$$

Thus, we have

$$\begin{aligned}\mathrm{Re}\left(\frac{\mathrm{d}\lambda}{\mathrm{d}\tau}\right)^{-1} &= \mathrm{Re}\left(-\frac{3\lambda^2 + 2p_2\lambda + p_1}{\lambda(\lambda^3 + p_2\lambda^2 + p_1\lambda + p_0)}\right)\Bigg|_{\lambda=i\omega_0} + \mathrm{Re}\left(\frac{q_1}{\lambda(q_1\lambda + q_0)}\right)\Bigg|_{\lambda=i\omega_0} \\ &= \frac{3\omega_0^4 + 2(p_2^2 - 2p_1)\omega_0^2 + p_1^2 - 2p_0p_2}{(\omega_0^3 - p_2\omega_0^2)^2 + (p_0 - p_2\omega_0^2)^2} - \frac{q_1^2}{q_1^2\omega_0^2 + q_0^2}.\end{aligned} \tag{3.8}$$

From Eq. (3.3) and Eq. (3.8), we can get

$$\begin{aligned}\mathrm{sign}\left\{\left.\frac{\mathrm{dRe}(\lambda)}{\mathrm{d}\tau}\right|_{\lambda=i\omega_0}\right\} &= \mathrm{sign}\left\{\mathrm{Re}\left(\frac{\mathrm{d}\lambda}{\mathrm{d}\tau}\right)^{-1}\right\}\Bigg|_{\lambda=i\omega_0} \\ &= \frac{3(\omega_0^2)^2 + 2e_{12}\omega_0^2 + e_{11}}{q_1^2\omega_0^2 + q_0^2} \\ &= \frac{U'(\omega_0^2)}{q_1^2\omega_0^2 + q_0^2} \\ &\neq 0.\end{aligned}$$

It follows that $\left.\frac{\mathrm{dRe}(\lambda)}{\mathrm{d}\tau}\right|_{\lambda=i\omega_0} \neq 0$ which marks the completion of the proof. □

Combining Lemmas 3.1–3.2 with the Hopf bifurcation theorem presented in [7], the following results are obtained.

Theorem 3.1. *For system (1.2),*

1. *If (H_2) is satisfied, then the positive equilibrium $E_4 = (x^*, y^*, g^*)$ maintains local asymptotic stability for all values of $\tau \geq 0$.*
2. *If (H_3) or (H_4) and (H_5) hold, then the positive equilibrium $E_4 = (x^*, y^*, g^*)$ exhibits local asymptotic stability for any $\tau \in [0, \tau_0)$ and is unstable for $\tau > \tau_0$. Furthermore, a Hopf bifurcation occurs at the positive equilibrium $E_4 = (x^*, y^*, g^*)$ in system (1.2) when $\tau = \tau_0$.*

3.2. Direction and stability of Hopf bifurcation

In this part, for system (1.2), we focus on determining the direction of Hopf bifurcation as well as the stability of the bifurcating periodic solutions by using normal form theory and center manifold theorem [7]. From the preceding analysis, we have already obtained that a Hopf bifurcation occurs in system (1.2) when $\tau = \tau_0$.

To transform without losing generality, let $\zeta = \tau - \tau_0, \zeta \in \mathbb{R}, t = r\tau, x(r\tau) = \hat{x}(r), y(r\tau) = \hat{y}(r), g(r\tau) = \hat{g}(r)$, where $x = \hat{x}$, $y = \hat{y}$, $g = \hat{g}$ and $t = r$, then system (1.2) can be expressed in the form of a functional differential equation in $C = C([-1, 0], \mathbb{R}^3)$:

$$\dot{R}(t) = L_\zeta(R_t) + f(\zeta, R_t), \tag{3.9}$$

where $R(t) = (x(t), y(t), g(t))^T \in C$, $R_t(\theta) = R(t + \theta) = (x(t + \theta), y(t + \theta), g(t + \theta))^T \in C$, and $L_\zeta : C \to \mathbb{R}^3$, $f : \mathbb{R} \times C \to \mathbb{R}^3$ are expressed as

$$L_\zeta(\phi) = (\tau_0 + \zeta)\{\bar{A}\phi(0) + \bar{B}\phi(-1)\}, \tag{3.10}$$

and

$$f(\zeta, \phi) = (\tau_0 + \zeta)(f_1, f_2, f_3)^T,$$

where

$$\begin{aligned}
&\phi(\theta) = (\phi_1(\theta), \phi_2(\theta), \phi_3(\theta))^T \in C,\\
&\bar{A} = \begin{pmatrix} a_{11}\, a_{12}\, a_{13} \\ a_{21}\, a_{22}\, a_{23} \\ a_{31}\, a_{32}\, a_{33} \end{pmatrix}, \quad \bar{B} = \begin{pmatrix} 0\, b_{12}\, 0 \\ 0\ \ 0\ \ 0 \\ 0\ \ 0\ \ 0 \end{pmatrix},\\
&f_1 = k_{11}\phi_1^2(0) + k_{12}\phi_1(0)\phi_2(0) + k_{13}\phi_1(0)\phi_2(-1) + k_{14}\phi_2^2(-1) + k_{15}\phi_2^2(0) + \cdots,\\
&f_2 = k_{21}\phi_1^2(0) + k_{22}\phi_1(0)\phi_2(0) + k_{23}\phi_2^2(0) + \cdots,\\
&f_3 = 0,
\end{aligned}$$

with

$$\begin{aligned}
k_{11} &= -\frac{r_1}{(k_1 - s_1 g^*)(1 + ky^*)} + \frac{my^{*2}(1 + w)^2(\alpha + \beta y^* + dg^*)^2}{[(1 + w)(\alpha + \beta y^* + dg^*)x^* + my^*]^3},\\
k_{12} &= -\frac{y^* m(1 + w)(2\alpha + 3\beta y^* + 2dg^*)}{[(1 + w)(\alpha + \beta y^* + dg^*)x^* + my^*]^2} + \frac{2\,[(1 + w)\beta x^* + m]\, my^*(1 + w)(\alpha + \beta y^* + dg^*)}{[(1 + w)(\alpha + \beta y^* + dg^*)x^* + my^*]^3},\\
k_{13} &= -\frac{kr_1\left(1 - \frac{2x^*}{k_1 - s_1 g^*}\right)}{(1 + ky^*)^2}, \quad k_{14} = \frac{k^2 r_1 x^*\left(1 - \frac{x^*}{k_1 - s_1 g^*}\right)}{(1 + ky^*)^3},\\
k_{15} &= \frac{x^*(1 + w)[(1 + w)\beta^2 x^* y^* + m(\alpha + \beta y^* + dg^*)]}{[(1 + w)(\alpha + \beta y^* + dg^*)x^* + my^*]^2}\\
&\quad - \frac{x^* y^*[(1 + w)\beta x^* + m]^2(\alpha + \beta y^* + dg^*)(1 + w)}{[(1 + w)(\alpha + \beta y^* + dg^*)x^* + my^*]^3},\\
k_{21} &= -\frac{e(1 + w)^2(\alpha + \beta y^* + dg^*)^2 my^{*2}}{[(1 + w)(\alpha + \beta y^* + dg^*)x^* + my^*]^3},
\end{aligned}$$

$$k_{22}=\frac{em(1+w)\left(2\alpha y^*+3\beta y^{*2}+2dg^*y^*\right)}{\left[(1+w)(\alpha+\beta y^*+dg^*)x^*+my^*\right]^2}-\frac{2\left[(1+w)\beta x^*+m\right](1+w)(\alpha+\beta y^*+dg^*)mey^{*2}}{\left[(1+w)(\alpha+\beta y^*+dg^*)x^*+my^*\right]^3},$$

$$k_{23}=-\frac{r_2}{k_2-s_2g^*}-\frac{ex^*(1+w)\left[(1+w)\beta^2x^*y^*+m(\alpha+\beta y^*+dg^*)\right]}{\left[(1+w)(\alpha+\beta y^*+dg^*)x^*+my^*\right]^2}$$
$$+\frac{ex^*y^*\left[(1+w)\beta x^*+m\right]^2(\alpha+\beta y^*+dg^*)(1+w)}{\left[(1+w)(\alpha+\beta y^*+dg^*)x^*+my^*\right]^3}.$$

According to the Riesz representation theorem [6], there exists a 3×3 matrix function $\eta(\theta,\zeta)$ when $\theta\in[-1,0]$, which is

$$L_\zeta(\phi)=\int_{-1}^{0}d\eta(\theta,\zeta)\phi(\theta),\quad \phi\in C([-1,0],\mathbb{R}^3). \tag{3.11}$$

In fact, we can take

$$\eta(\theta,\zeta)=(\tau_0+\zeta)\bar{A}\delta(\theta)+(\tau_0+\zeta)\bar{B}\delta(\theta+1) \tag{3.12}$$

and

$$\delta(\theta)=\begin{cases}0, & \theta\neq0,\\ 1, & \theta=0.\end{cases}$$

For $\phi\in C([-1,0],\mathbb{R}^3)$, make

$$A(\zeta)\phi=\begin{cases}\dfrac{d\phi(\theta)}{d\theta}, & -1\le\theta<0,\\ \displaystyle\int_{-1}^{0}d\eta(\theta,\zeta)\phi(\theta), & \theta=0,\end{cases} \tag{3.13}$$

and

$$B_\zeta(\phi)=\begin{cases}0, & -1\le\theta<0,\\ f(\zeta,\phi), & \theta=0.\end{cases} \tag{3.14}$$

Subsequently, Eq. (3.9) is able to be rewritten as

$$\dot{R}_t=A(\zeta)R_t+B(\zeta)R_t. \tag{3.15}$$

Let $\varphi\in C([-1,0],(\mathbb{R}^3)^*)$, with $(\mathbb{R}^3)^*$ representing the three-dimensional space of row vectors. The adjoint operator A^* of $A(0)$ is able to be expressed as

$$A^*\varphi(r)=\begin{cases}-\dfrac{d\varphi(r)}{dr}, & 0<r\le1,\\ \displaystyle\int_{-1}^{0}d\eta^T(1,0)\varphi(-r), & r=0.\end{cases} \tag{3.16}$$

For $\phi\in C([-1,0],\mathbb{R}^3)$ and $\varphi\in C([-1,0],(\mathbb{R}^3)^*)$, a bilinear form can be defined by

$$\langle\varphi(r),\phi(r)\rangle=\bar{\varphi}(0)\phi(0)-\int_{-1}^{0}\int_{\zeta=0}^{\zeta}\bar{\varphi}(\zeta-\theta)d\eta(\theta)\phi(\zeta)d\zeta, \tag{3.17}$$

where $\eta(\theta)=\eta(\theta,0)$, $A=A(0)$. By the discussion before, we can see that $\pm i\omega_0\tau_0$ are the eigenvalues of $A(0)$ and A^*.

Suppose $q(\theta) = (1, q_2, q_3)^T e^{i\omega_0\tau_0\theta}$ is the eigenvector of $A(0)$ associated with the eigenvalue $i\omega_0\tau_0$, and let $q^*(r) = \Omega(1, q_2^*, q_3^*)e^{i\omega_0\tau_0 r}$ be the eigenvector of A^* related to the eigenvalue $-i\omega_0\tau_0$. Through a careful calculation, we have

$$\begin{aligned}
q_2 &= \frac{a_{23}a_{31} + a_{21}(i\omega_0 - a_{33})}{(i\omega_0 - a_{22})(i\omega_0 - a_{33}) - a_{23}a_{32}},\\
q_3 &= \frac{a_{32}a_{21} + a_{31}(i\omega_0 - a_{22})}{(i\omega_0 - a_{22})(i\omega_0 - a_{33}) - a_{23}a_{32}},\\
q_2^* &= \frac{(i\omega_0 + a_{33})(i\omega_0 + a_{11}) - a_{13}a_{31}}{a_{31}a_{23} - (i\omega_0 + a_{33})a_{21}},\\
q_3^* &= \frac{a_{21}a_{13} - a_{23}(i\omega_0 + a_{11})}{a_{23}a_{31} - a_{21}(i\omega_0 + a_{33})}.
\end{aligned}$$

Then, from Eq. (3.17), we obtain

$$\begin{aligned}
\langle q^*(r), q(\theta)\rangle &= \bar{\Omega}(1, q_2^*, q_3^*)(1, q_2, q_3)^T - \int_{-1}^{0}\int_{\zeta=0}^{\theta} \bar{q}^*(\zeta - \theta)d\eta(\theta)\phi(\zeta)d\zeta\\
&= \bar{\Omega}\left(1 + \bar{q}_2^* q_2 + \bar{q}_3^* q_3 + \tau_0 e^{-i\omega_0\tau_0} q_2 b_{12}\right).
\end{aligned} \tag{3.18}$$

So, we select $\bar{\Omega} = \left(1 + \bar{q}_2^* q_2 + \bar{q}_3^* q_3 + \tau_0 e^{-i\omega_0\tau_0} q_2 b_{12}\right)^{-1}$ to satisfy the conditions $\langle q^*(r), q(\theta)\rangle = 1$ and $\langle q^*(r), \bar{q}(\theta)\rangle = 0$.

Next, let R_t represent the solution of Eq. (3.15) for $\zeta = 0$. We define

$$z(t) = \langle q^*, R_t\rangle,\ W(t, \theta) = R_t - zq - \bar{z}\bar{q} = R_t - 2\mathrm{Re}\{z(t)q(\theta)\}. \tag{3.19}$$

Upon analyzing the center manifold C_0, we get

$$W(t, \theta) = W(z(t), \bar{z}(t), \theta) = W_{20}(\theta)\frac{z^2}{2} + W_{11}(\theta)z\bar{z} + W_{02}(\theta)\frac{\bar{z}^2}{2} + \cdots, \tag{3.20}$$

where z and $\bar{z}$ are local coordinates for C_0 in the direction of q^* and $\bar{q}^*$. It should be noted that W takes real values when R_t takes real values, and our consideration is restricted to real solutions. From Eq. (3.19), we obtain

$$\langle q^*, W\rangle = \langle q^*, R_t - zq - \bar{z}\bar{q}\rangle = \langle q^*, R_t\rangle - \langle q^*, q\rangle z - \langle q^*, \bar{q}\rangle\bar{z}.$$

Considering a solution $R_t \in C_0$ formed by Eqs (3.11), (3.15), (3.16) and $\zeta = 0$, we get

$$\begin{aligned}
\dot{z}(t) &= \langle q^*, \dot{R}_t\rangle = \langle q^*, A(0)R_t + B(0)R_t\rangle\\
&= \langle A^*(0)q^*, R_t\rangle + \langle \bar{q}^*(0)f(0), R_t\rangle\\
&:= i\omega_0\tau_0 z(t) + \bar{q}^*(0)f_0(z, \bar{z}).
\end{aligned} \tag{3.21}$$

Then, Eq. (3.21) admits the following rewritten form:

$$\dot{z}(t) = i\omega_0\tau_0 z(t) + g(z, \bar{z}), \tag{3.22}$$

where

$$g(z, \bar{z}) = g_{20}\frac{z^2}{2} + g_{11}z\bar{z} + g_{02}\frac{\bar{z}^2}{2} + g_{21}\frac{z^2\bar{z}}{2} + \cdots. \tag{3.23}$$

Then by a similar computation process in [35], to further explore the direction and stability of Hopf bifurcation, we obtain the following relevant parameters:

$$
\begin{aligned}
g_{20} &= 2\tau_0\bar{\Omega}\left[k_{11}+k_{12}q_2+k_{13}q_2e^{-i\omega_0\tau_0}+k_{14}q_2^2e^{-2i\omega_0\tau_0}+k_{15}q_2^2+\bar{q}_2^*(k_{21}+k_{22}q_2+k_{23}q_2^2)\right],\\
g_{11} &= \tau_0\bar{\Omega}\left\{2k_{11}+k_{12}(\bar{q}_2+q_2)+k_{13}\left(\bar{q}_2e^{i\omega_0\tau_0}+q_2e^{-i\omega_0\tau_0}\right)+2k_{14}q_2\bar{q}_2+2k_{15}q_2\bar{q}_2\right.\\
&\quad \left.+\bar{q}_2^*\left[2k_{21}+k_{22}(\bar{q}_2+q_2)+2k_{23}q_2\bar{q}_2\right]\right\},\\
g_{02} &= 2\tau_0\bar{\Omega}\left[k_{11}+k_{12}\bar{q}_2+k_{13}\bar{q}_2e^{i\omega_0\tau_0}+k_{14}\bar{q}_2{}^2e^{2i\omega_0\tau_0}+k_{15}\bar{q}_2^2+\bar{q}_2^*\left(k_{21}+k_{22}\bar{q}_2+k_{23}\bar{q}_2^2\right)\right],\\
g_{21} &= 2\tau_0\bar{\Omega}\left\{k_{11}\left(2W_{11}^{(1)}(0)+W_{20}^{(1)}(0)\right)+k_{12}\left(W_{11}^{(2)}(0)+\frac{W_{20}^{(2)}(0)}{2}+\frac{\bar{q}_2}{2}W_{20}^{(1)}(0)+q_2W_{11}^{(1)}(0)\right)\right.\\
&\quad +k_{13}\left(W_{11}^{(2)}(-1)+\frac{W_{20}^{(2)}(-1)}{2}+\frac{e^{i\omega_0\tau_0}}{2}W_{20}^{(1)}(0)\bar{q}_2+W_{11}^{(1)}(0)e^{-i\omega_0\tau_0}q_2\right)\\
&\quad +k_{14}\left(e^{i\omega_0\tau_0}W_{20}^{(2)}(-1)\bar{q}_2+2W_{11}^{(2)}(-1)e^{-i\omega_0\tau_0}q_2\right)+k_{15}\left(\bar{q}_2W_{20}^{(2)}(0)+2q_2W_{11}^{(2)}(0)\right)\\
&\quad +\bar{q}_2^*\left[k_{21}\left(2W_{11}^{(1)}(0)+W_{20}^{(1)}(0)\right)+k_{22}\left(W_{11}^{(2)}(0)+\frac{W_{20}^{(2)}(0)}{2}+\frac{\bar{q}_2}{2}W_{20}^{(1)}(0)+q_2W_{11}^{(1)}(0)\right)\right.\\
&\quad \left.\left.+k_{23}\left(\bar{q}_2W_{20}^{(2)}(0)+2q_2W_{11}^{(2)}(0)\right)\right]\right\}.
\end{aligned}
$$

We can also have

$$
\begin{aligned}
W_{20}(\theta) &= \frac{ig_{20}}{\omega_0\tau_0}q(0)e^{i\omega_0\tau_0\theta}+\frac{i\bar{g}_{02}}{3\omega_0\tau_0}\bar{q}(0)e^{-i\omega_0\tau_0\theta}+F_1e^{2i\omega_0\tau_0\theta},\\
W_{11}(\theta) &= -\frac{ig_{11}}{\omega_0\tau_0}q(0)e^{i\omega_0\tau_0\theta}+\frac{i\bar{g}_{11}}{\omega_0\tau_0}\bar{q}(0)e^{-i\omega_0\tau_0\theta}+F_2,
\end{aligned}
$$

where $F_1=(F_1^{(1)},F_1^{(2)},F_1^{(3)})^T\in\mathbb{R}^3$ and $F_2=(F_2^{(1)},F_2^{(2)},F_2^{(3)})^T\in\mathbb{R}^3$ are constant vectors and they can be expressed through the equations below:

$$
\begin{pmatrix}
2i\omega_0-a_{11} & -a_{12}-b_{12}e^{-2i\omega_0\tau_0} & -a_{13}\\
-a_{21} & 2i\omega_0-a_{22} & -a_{23}\\
-a_{31} & -a_{32} & 2i\omega_0-a_{33}
\end{pmatrix}F_1=2\begin{pmatrix}H_1\\H_2\\H_3\end{pmatrix},
$$

$$
\begin{pmatrix}
-a_{11} & -a_{12}-b_{12} & -a_{13}\\
-a_{21} & -a_{22} & -a_{23}\\
-a_{31} & -a_{32} & -a_{33}
\end{pmatrix}F_2=\begin{pmatrix}P_1\\P_2\\P_3\end{pmatrix},
$$

where

$$
\begin{aligned}
H_1 &= k_{11}+k_{12}q_2+k_{13}q_2e^{-i\omega_0\tau_0}+k_{14}q_2^2e^{-2i\omega_0\tau_0}+k_{15}q_2^2,\\
H_2 &= k_{21}+k_{22}q_2+k_{23}q_2^2,\\
H_3 &= 0,\\
P_1 &= 2k_{11}+k_{12}(\bar{q}_2+q_2)+k_{13}\left(\bar{q}_2e^{i\omega_0\tau_0}+q_2e^{-i\omega_0\tau_0}\right)+2k_{14}q_2\bar{q}_2+2k_{15}q_2\bar{q}_2,\\
P_2 &= 2k_{21}+k_{22}(\bar{q}_2+q_2)+2k_{23}q_2\bar{q}_2,\\
P_3 &= 0.
\end{aligned}
$$

Therefore, we can determine the coefficient g_{21}. Furthermore, we have the following values:

$$
\begin{aligned}
c_1(0) &= \frac{i}{2\omega_0\tau_0}\left(g_{20}g_{11} - 2|g_{11}|^2 - \frac{|g_{02}|^2}{3}\right) + \frac{g_{21}}{2},\\
\mu_2 &= -\frac{\mathrm{Re}\{c_1(0)\}}{\mathrm{Re}\{\lambda'(\tau_0)\}},\\
\beta_2 &= 2\mathrm{Re}\{c_1(0)\},\\
T_2 &= -\frac{\mathrm{Im}\{c_1(0)\} + \mu_2\mathrm{Im}\{\lambda'(\tau_0)\}}{\omega_0\tau_0},
\end{aligned}
$$

which decide the properties of bifurcating periodic solutions when $\tau = \tau_0$.

We can draw the conclusions below according to the preceding discussion.

Theorem 3.2. *For system (1.2),*

(1) The direction of Hopf bifurcation is decided by the sign of μ_2. Specifically, the Hopf bifurcation is supercritical (subcritical) if $\mu_2 > 0$ ($\mu_2 < 0$).

(2) The stability of bifurcating periodic solutions is decided by the sign of β_2. In other words, the bifurcating periodic solutions are unstable (stable) when $\beta_2 > 0 (< 0)$.

(3) The sign of T_2 decides the period of bifurcating periodic solutions. When $T_2 > 0 (< 0)$, the bifurcating periodic solutions express increase (decrease).

Table 2. The number and stability of positive equilibria under different parameter conditions.

Parameter value	Number of positive equilibria	Stability of equilibria
$d = 0.2, s_2 = 2.3, w = 0.5$	E_1^*, E_2^*, E_3^*	E_1^* is stable and E_2^*, E_3^* are unstable.
$s_2 = 2.3, w = 1$	E_1^*, E_2^*, E_3^*	E_1^* is unstable and E_2^*, E_3^* are stable.
$s_1 = 0.5, s_2 = 2.3, w = 1$	E_1^*, E_2^*	E_1^* is stable and E_2^* is unstable.
$s_1 = 0.1, s_2 = 2, w = 1$	E_1^*, E_2^*	Both are unstable.
$s_1 = 1, s_2 = 2, w = 1$	E_1^*	Unstable
Unchanged	E_1^*	Stable

4. Numercial simulation

In this section, to support the theoretical results, we will present numerical simulations and give related biological explanations.

With the parameters taken from Table 1, through calculations, we obtain an unstable extinction equilibrium $E_1 = (0, 0, 0.5)$ and an unstable predator free equilibrium $E_2 = (6.8571, 0, 3.9286)$. To ensure the existence of the prey free equilibrium, we set $d_1 = 0.1$, while the values of other parameters remain unchanged in Table 1. Then, we get the prey free equilibrium $E_3 = (0, 2.1354, 3.7031)$ which is stable. Next, in Table 2, we select some parameter values to investigate the number and stability of interior equilibria, where the other parameters remain consistent with Table 1. For convenience, we use E_1^*, E_2^*, and E_3^* to represent different positive equilibria. From Table 2, it is obvious that under specific parameter conditions, the system can converge to different stable states when different initial conditions are adopted.

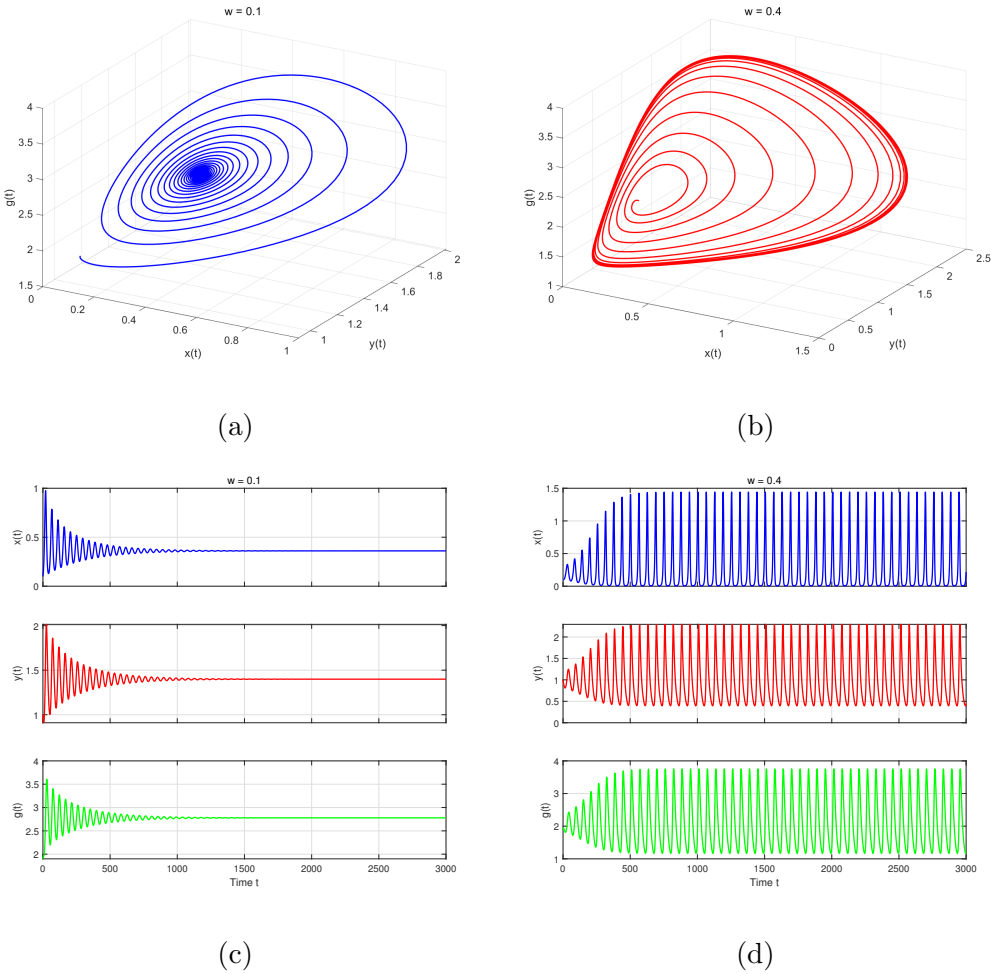

Figure 2. Phase portraits and time-series plots for different values of w.

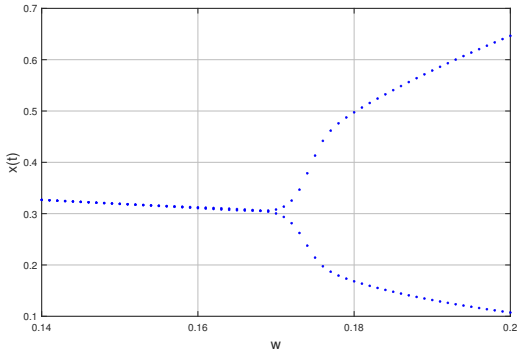

Figure 3. Bifurcation diagram of system (2.1) with respect to w.

For the non-delayed system (2.1), first, we choose w as a parameter to study the impact of wind flow. Let $k = 0.2, d = 0.2$ and other parameters be the same as Table 1. We take different values of w to observe the stability of the system. Making $w = 0.1$, we can find that the system

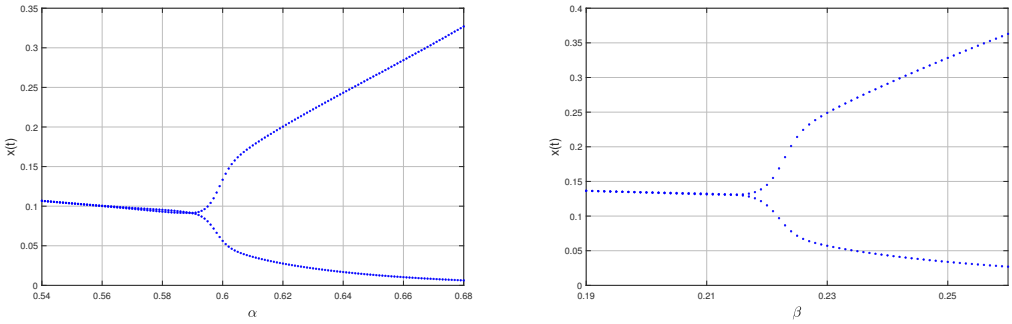

(a) (b)

Figure 4. Bifurcation diagrams of system (2.1). (a) Hopf bifurcation diagram in the $\alpha - x$ plane. (b) Hopf bifurcation diagram in the $\beta - x$ plane.

is stable according to the phase portrait (a) in Figure 2. The corresponding time-series plot in Figure 2(c) further confirms this stability. From the time-series plot, the system exhibits oscillatory dynamics until $t = 1000$; beyond $t = 1000$, the system reverts to a stable state. Then we let $w = 0.4$. The simulation shows that the system becomes unstable and shows periodic cycles, as illustrated in Figure 2(b) and (d). This indicates that with other ecological parameters taking the aforementioned fixed values, an increase in wind flow can change the stability of the system (2.1) and lead to the occurrence of a Hopf bifurcation. As the value of w increases and reaches $w_H = 0.1680$, the system undergoes a Hopf bifurcation and generates limit cycles, as shown in Figure 3. From an ecological perspective, an increase in wind flow can induce the emergence of limit cycles in the system, leading to population oscillations. When $w < w_H$, the species can coexist. In other words, the effect of wind speed on predation efficiency is crucial for the realization of population coexistence.

Next, we take α as bifurcation parameter to examine the impact of hunting cooperation on populations, while keeping the other parameters the same as in Table 1, except for $d = 0.2$. As shown in Figure 4(a), the system undergoes a Hopf bifurcation at $\alpha = 0.5894$. Then, select β as bifurcation parameter under the same parameter conditions. As shown in Figure 4(b), the system undergoes a Hopf bifurcation at $\beta = 0.2141$. For subsequent analysis, we focus on the parameter β to further investigate the influence of hunting cooperation. As shown in Figure 5, the system is stable when $\beta = 0.1$. When $\beta = 0.8$, periodic oscillations occur. Ecologically speaking, moderate hunting cooperation facilitates the maintenance of a steady state for species, whereas excessive cooperation can lead to system oscillations. This implies that artificial intervention is required to ensure the stability of the system when the level of cooperation reaches a critical value.

To study the impact of the death rate of predators, we keep the other parameters the same as Table 1 and select the death rate of predator d_1 as the bifurcation parameter. According to Figure 6, the system (2.1) experiences a transcritical bifurcation at $d_1 = d_{1t} = 0.17$, which is consistent with Theorem 2.3. When $d_1 > 0.17$, the interior equilibrium E_4 is stable and the species coexist. When $d_1 < 0.17$, the extinction equilibrium E_1 is unstable and the predator populations go extinct, which means that the equilibria change stability at $d_1 = d_{1t}$. Obviously, when the death rate of predators is relatively high, the system can still recover to a coexistence state even if there are short-term fluctuations in the species population.

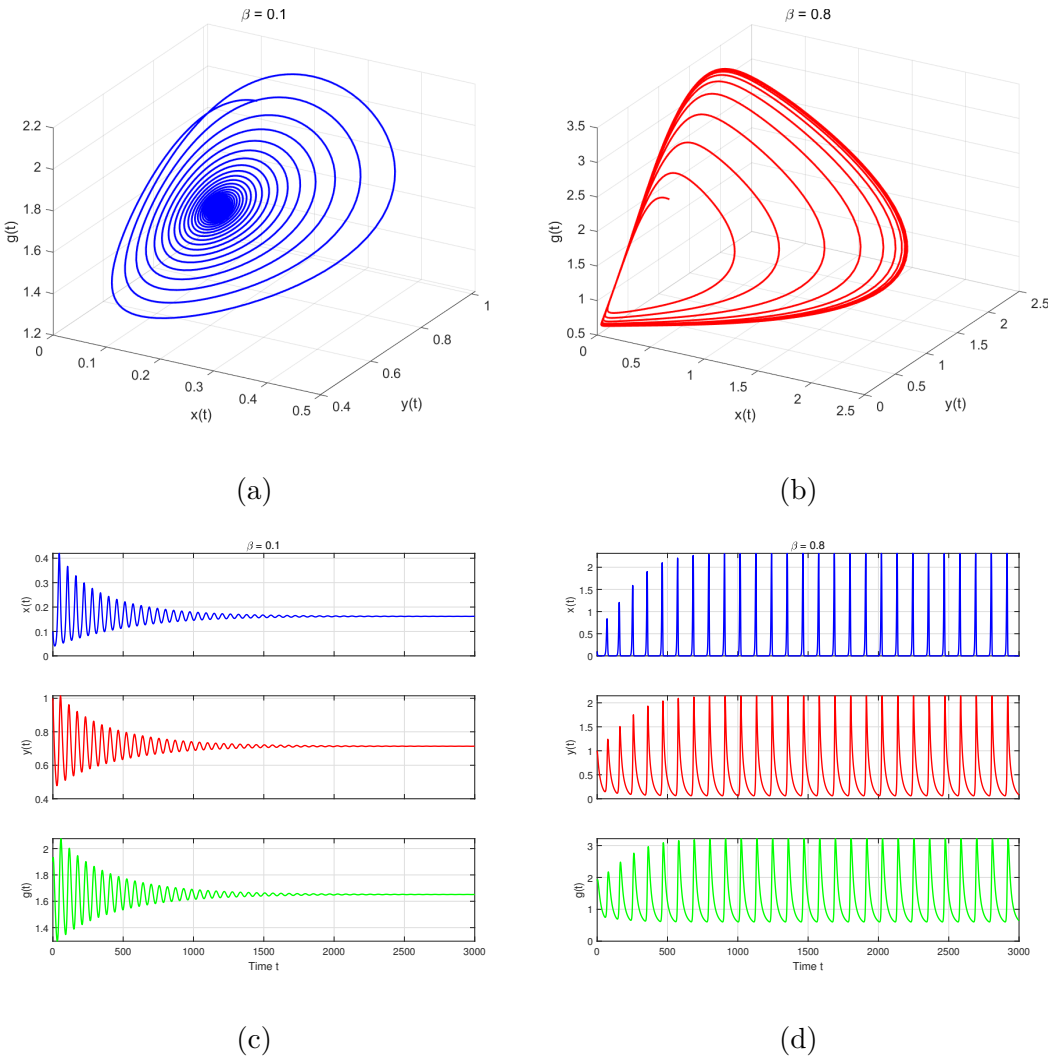

Figure 5. Phase portraits and time-series plots for different values of β.

Then, we investigate the effect of global warming on system (2.1). We choose s_2 as the bifurcation parameter and make $s_1 = 0.6, d = 0.2, k = 0.2, m = 4$, while the other parameters remain unchanged with Table 1. Figure 7(a) shows that the system (2.1) undergoes a transcritical bifurcation at $s_2 = 5.0262$, where the system experiences an exchange of stability between equilibria. When s_2 is less than the critical value, E_3 is unstable and E_4 is stable, allowing predators and prey to coexist. When $s_2 > 5.0262$, E_3 is stable and E_4 becomes unstable. Next, making $s_1 = 0.6, d = 0.2, k = 0.2$, while the other parameters remain unchanged with Table 1, we take different values of s_2 to observe the stability of the system. According to Figure 8, the system is unstable when $s_2 = 0.4$ and stable when $s_2 = 1.3$. This indicates that, system (2.1) undergoes a Hopf bifurcation while the value of s_2 increases (see Figure 7(b)). By calculation, we find that a Hopf bifurcation occurs at $s_2 = 1.0839$. Keeping the other parameters the same as in Table 1, except for $s_2 = 1, d = 0.2, k = 0.2$, we choose s_1 as the bifurcation parameter and find that the system (2.1) undergoes a Hopf bifurcation at $s_1 = 0.8717$. We observe that an increase in either parameter s_1 or s_2 drives the system to shift from an unstable oscillatory state to a

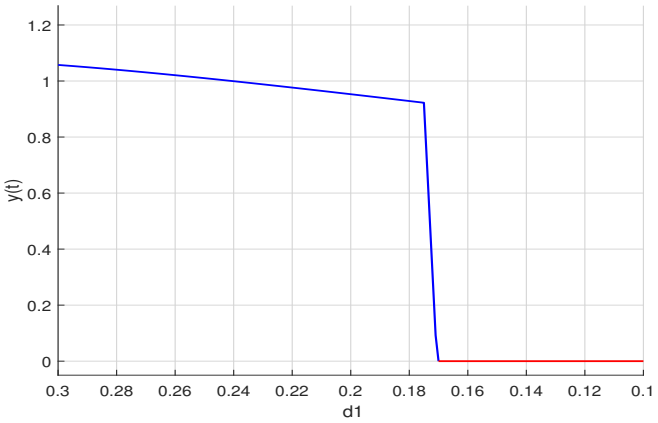

Figure 6. The transcritical bifurcation diagram of system (2.1) for bifurcation parameter d_1.

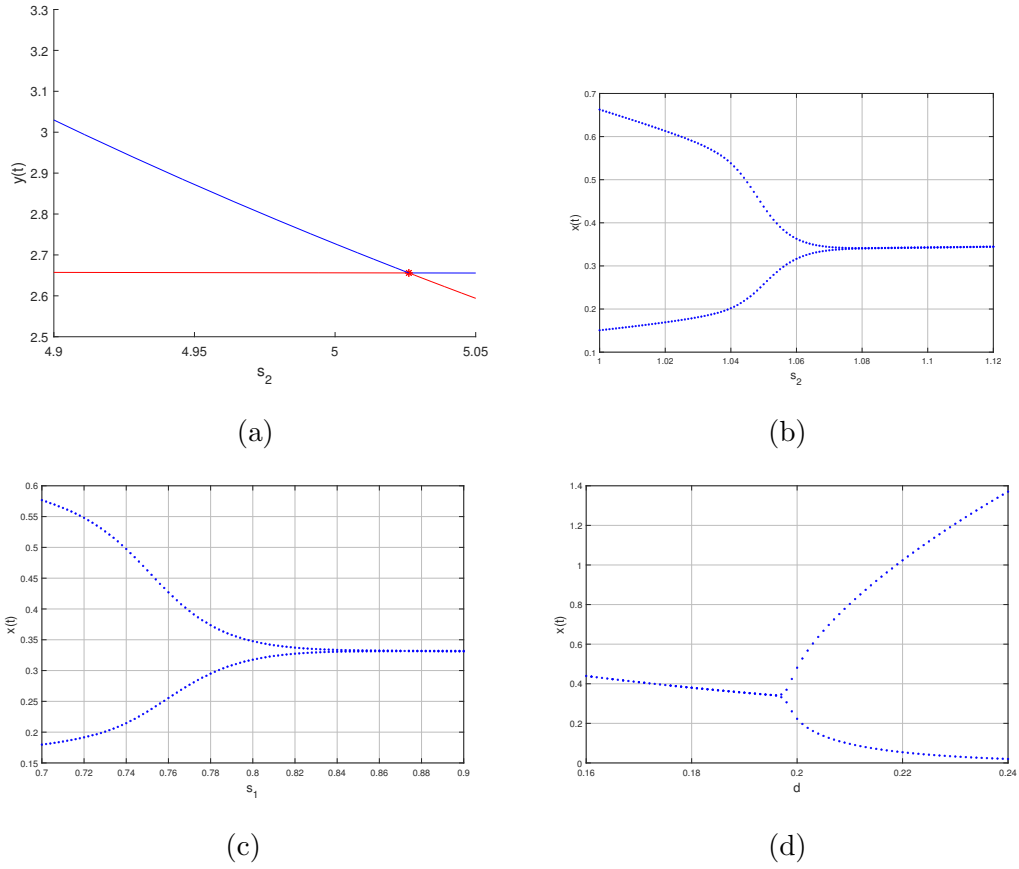

Figure 7. Bifurcation diagrams of system (2.1). (a) Transcritical bifurcation diagram in the $s_2 - y$ plane. (b) Hopf bifurcation diagram in the $s_2 - x$ plane. (c) Hopf bifurcation diagram in the $s_1 - x$ plane. (d) Hopf bifurcation diagram in the $d - x$ plane.

stable coexistence state. Next, d is selected as the bifurcation parameter with $s_2 = 1, k = 0.2$, while the other parameters remain the same as in Table 1. As shown in Figure 7(d), the system

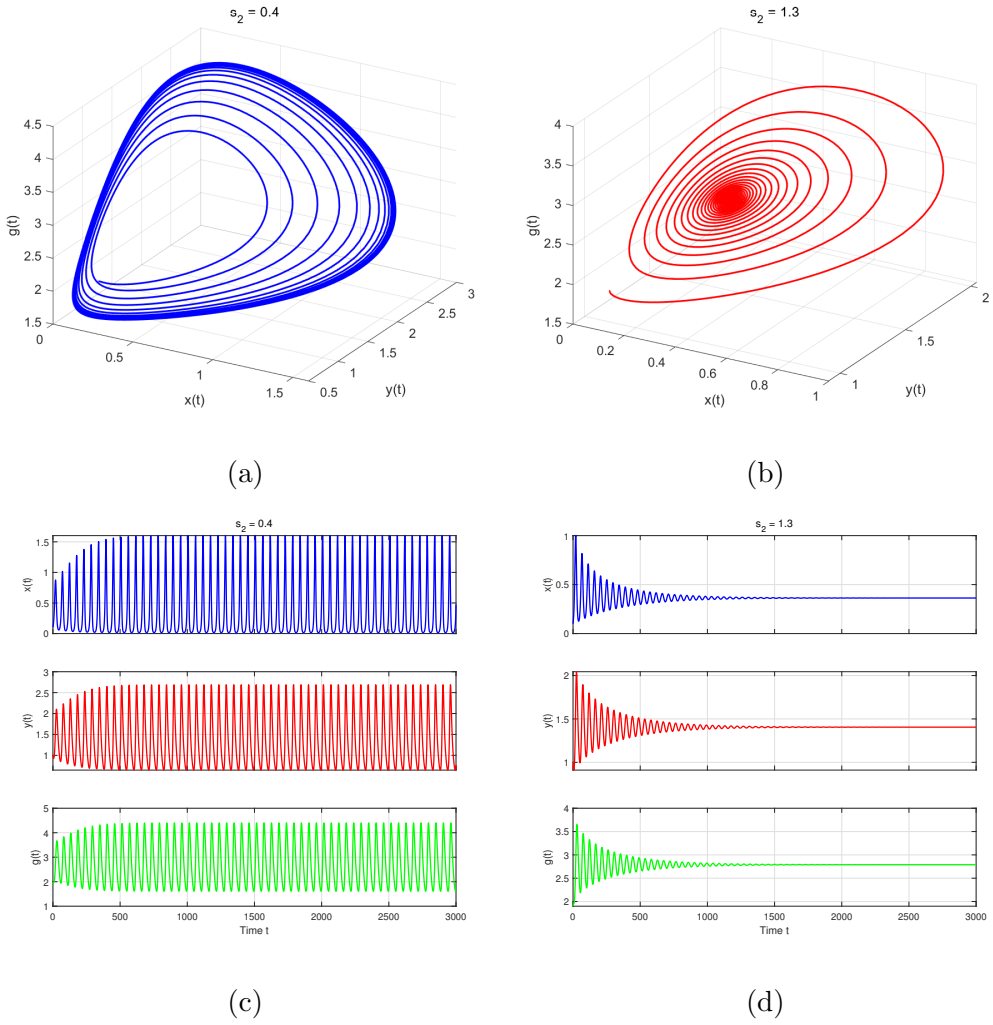

Figure 8. Phase portraits and time-series plots for different values of s_2.

undergoes a Hopf bifurcation at $d = 0.1984$, and increasing the parameter d leads the system to transition from a stable state to an unstable state. From an ecological perspective, the stronger the impact of global warming on the predation process, the more difficult it is for species to coexist. In contrast, intensifying global warming reduces the carrying capacity of the population, thereby limiting the size of the predator population and making oscillations more difficult to occur.

Finally, we concentrate on investigating the impact of fear on populations. We consider k as a parameter and maintain the values of the remaining parameters the same as in Table 1. From Figure 9, a rise in the value of k usually results in lower densities for both the prey and the predator. Ecologically speaking, as the level of fear intensifies, prey adopt more anti-predator strategies, which consequently suppresses their own reproductive rate. As a result, the density of the prey population decreases. Due to the food crisis caused by the prey, the population size of the predator decreases accordingly.

For the delayed system (1.2), we use the same parameter values in Table 1. Then the unique interior equilibrium $E_4(0.2873, 0.9529, 2.0730)$ can be easily obtained.

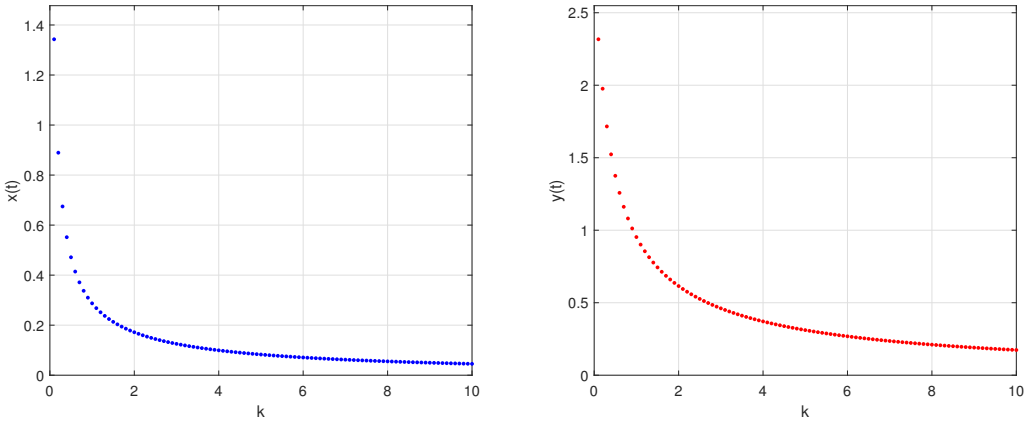

(a) (b)

Figure 9. The dependence of populations on k. (a) $x(t)$, (b) $y(t)$.

When $\tau = 0$, we can obtain $p_{12} > 0, p_{10} > 0, p_{12}p_{11} > p_{10}$. Therefore, condition (H_1) is satisfied, which means that E_4 is local asymptotic stability.

When $\tau \neq 0$, through further calculations, we get $\omega_0 = 0.1111, \tau_0 = 3.4863$. According to Theorem 3.1, we find that E_4 possesses local asymptotic stability in the case of $\tau = 2 < \tau_0$, which is evident in Figure 10(a). When the fear response delay exceeds the critical value of τ_0, E_4 loses its stability (see Figure 10(b)). Moreover, system (1.2) experiences a Hopf bifurcation at E_4 when the value of τ reaches $\tau_0 = 3.4863$ (see Figure 10(c)), which means periodic solutions bifurcate from E_4. From the ecological point of view, if the fear response delay below the critical value, species can coexist over an extended period. When the delay crosses the critical value, species still maintain positive population densities but exhibit periodic oscillations.

Assessing the sensitivity of the system with respect to initial conditions holds significant value. Given the parameter values outlined in Table 1, we select $\tau = 2$ and $\tau = 4$, which are capable of stabilizing and destabilizing the positive equilibrium of system (1.2). Subsequently, we introduce minor modifications to the original initial conditions and generate phase diagrams for distinct initial values $(0.1, 1.1, 2.0)$, $(0.1, 1.2, 2.1)$, $(0.1, 1.0, 1.9)$, as depicted in Figure 11. It is evident that even though slight variations in initial values induce changes in population quantities during the early evolution of species, they do not affect the ultimate state of the two populations.

At last, we discuss the properties of the Hopf bifurcation at E_4. Through further calculations, we get $c_1(0) = -1.6445 - 0.0044i$, $\mu_2 = 484.0980$, $\beta_2 = -3.2889$, $T_2 = 1.6184$. According to the conclusions of Theorem 3.2, the Hopf bifurcation is supercritical, the bifurcating periodic solutions possess stability, and the period of the bifurcation periodic solutions is increasing. By studying the changes in the real and imaginary parts of E_4, we get E_4 is stable if $\tau < \tau_0$ and unstable if $\tau > \tau_0$. The system transitions from a stable equilibrium to an unstable equilibrium while generating stable bifurcation periodic solutions, which confirms the bifurcation is supercritical. From a biological perspective, this implies that even as time delays increase, species can still achieve coexistence through dynamic regulation, thereby preventing the extinction of a single species. Furthermore, when subjected to short-term external disturbances, the periodic oscillations of populations can still revert to their original patterns.

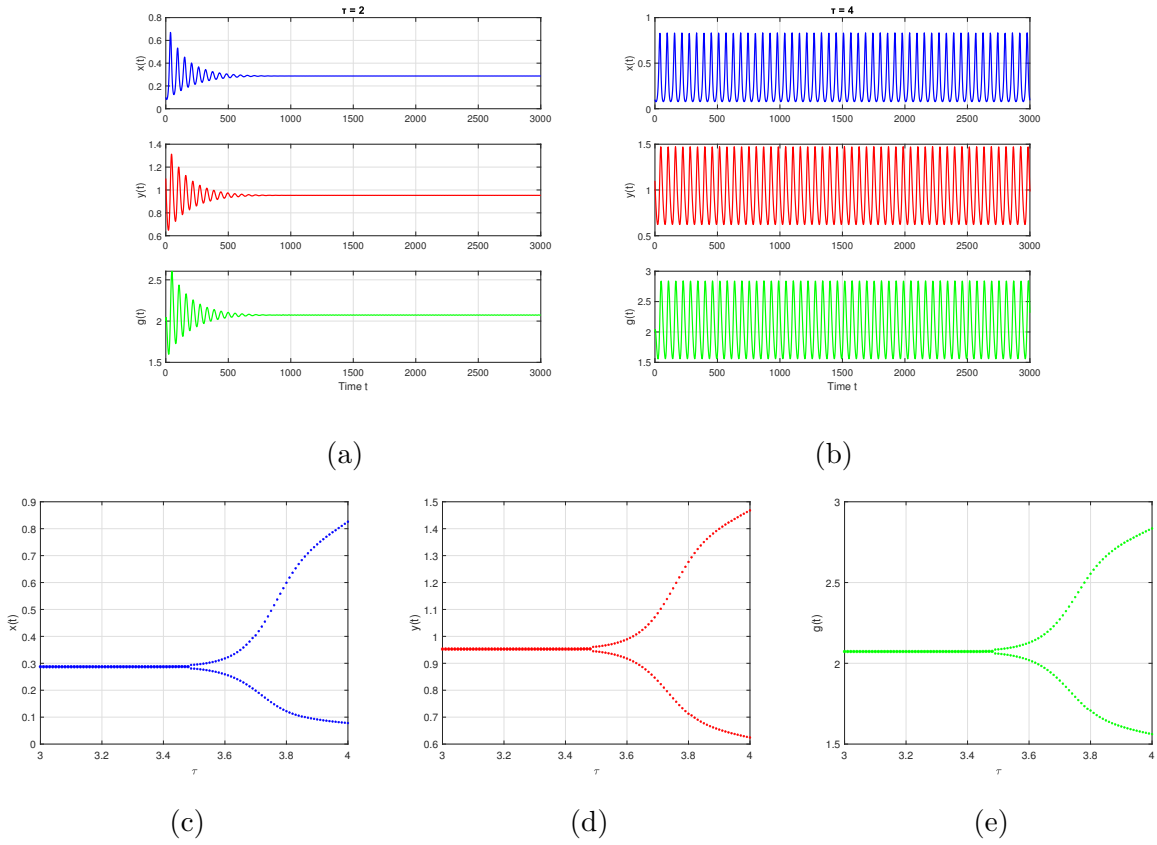

Figure 10. Time-series plots and bifurcation diagrams with respect to fear response delay.

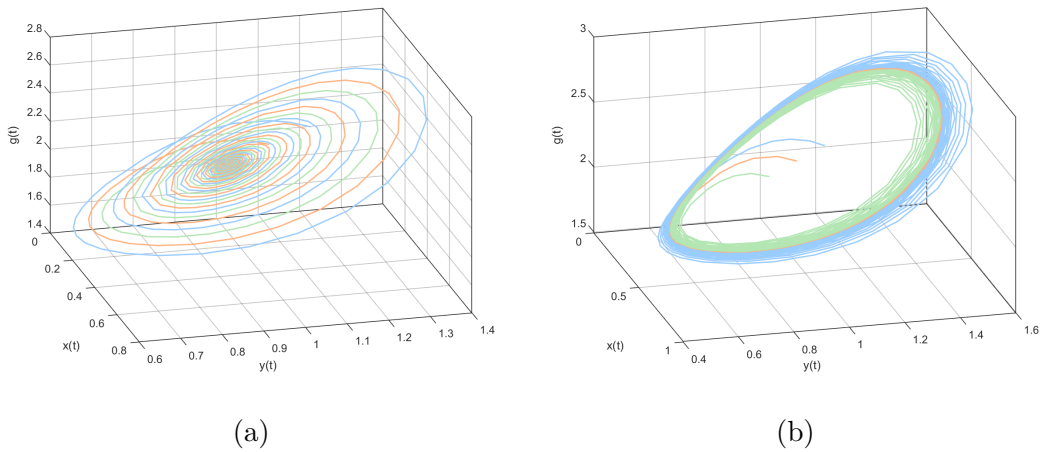

Figure 11. Sensitivity of solutions of the system (1.2) regarding the initial conditions. Orange, blue, and green curves represent the initial conditions $(0.1, 1.1, 2.0)$, $(0.1, 1.2, 2.1)$ and $(0.1, 1.0, 1.9)$, respectively. (a) $\tau = 2$, (b) $\tau = 4$.

5. Conclusion

In this paper, we investigate a Lotka-Volterra model incorporating global warming, wind, hunting cooperation, and fear effect. In addition, a time delay is introduced to represent the response time of the prey upon perceiving the risk of predation.

First, we confirm the well-posedness of the non-delayed system (2.1) by proving the positivity and boundedness of the solutions. The positivity of solutions ensures that population densities remain non-negative at all times, while the boundedness reflects the constraint of limited natural resources, preventing unrealistic infinite growth of populations. Subsequently, we derive the existence conditions for four equilibria. For system (2.1), we use the Routh-Hurwitz criterion to discuss the local stability of the four equilibria. Then, we analyze the existence of transcritical bifurcation and Hopf bifurcation at different equilibria. Furthermore, we examine the existence and properties of Hopf bifurcation for system (1.2) and carry out the numerical simulations. Our findings are summarized as follows.

For system (2.1), we first examine the effect of wind, and find that a Hopf bifurcation occurs in the system at $w = 0.1680$. Excessive high wind speed induces the emergence of limit cycles in the system, making it difficult for species to achieve stable coexistence. Next, we examine the effect of hunting cooperation. When α is chosen as the bifurcation parameter, a Hopf bifurcation can be observed in the system. Similarly, a Hopf bifurcation also occurs when β is taken as the bifurcation parameter. We find that moderate cooperation can increase the population size of predators, yet an excessively high level of cooperation will destabilize the system and render species coexistence unattainable. In addition, when d_1 is selected as the bifurcation parameter, we find system (2.1) experiencing a transcritical bifurcation, which means an extremely low predator mortality rate can drive the system to the brink of extinction. We further explore the impacts of global warming on the environmental carrying capacity and predation process. When s_1 is taken as the bifurcation parameter, a Hopf bifurcation occurs at $s_1 = 0.8717$. Similarly, a Hopf bifurcation occurs at $s_2 = 1.0839$ when s_2 is chosen as the bifurcation parameter. These two parameters have comparable effects on the system dynamics. Nevertheless, under another parameter conditions, increasing s_2 triggers a stability exchange between E_3 and E_4, which means system (2.1) undergoes a transcritical bifurcation. Within a certain range, a small value of d is more conducive to maintaining system stability. However, when s_1 or s_2 is small, system (2.1) shows periodic oscillations. Finally, with respect to the fear effect k, we observe that an increase in k leads to a decline in the population sizes of both prey and predators. This indicates that intense fear pressure exerts an adverse impact on the reproduction of both prey and predator populations, while the steady state of the system remains unchanged.

For system (1.2), we study the Hopf bifurcation by taking the time delay as a bifurcation parameter. Through numerical simulations, we find that system (1.2) undergoes a Hopf bifurcation at $\tau_0 = 3.4863$. When $\tau = 2 < \tau_0$, system (1.2) is locally asymptotically stable at E_4. When $\tau = 4 > \tau_0$, system (1.2) becomes unstable. In other words, when $\tau < \tau_0$, species can maintain a relatively stable coexistence state. Conversely, when $\tau > \tau_0$, the originally stable coexistence state of species is disrupted, which increases the risk of local population decline or even temporary disappearance, thereby threatening the resilience of the entire ecosystem. Additionally, we explore the properties of the Hopf bifurcation by applying the normal form theory and the center manifold theorem. Through a series of calculations, we obtain that the Hopf bifurcation is supercritical and the periodic solutions from the Hopf bifurcation are stable.

Findings indicate that wind, hunting cooperation, global warming and fear response delay can all induce Hopf bifurcation in the above systems. Among these factors, global warming

exerts multifaceted effects on the system. Intensifying global warming reduces the environmental carrying capacity of species. When global warming is mild, species exhibit a high carrying capacity and the system remains in an oscillatory state. As global warming increases and the carrying capacity decreases, the population density tends to stability. However, under certain conditions, the coexist equilibrium switches from stable to unstable when s_2 intensifies beyond the critical value 5.0262. This is consistent with the current ecological reality that global warming exerts significant impacts on ecosystem stability, as many species depend on specific temperature thresholds and habitats. The fear effect can directly reduce the density of prey, which causes a decline in predator populations due to food shortages. This indicates that excessive fear pressure is detrimental to species. The existence of fear response delay reflects the lag effect of ecosystem responses to fear. When the delay is within a reasonable range, populations can remain stable. However, an excessively long lag will trigger periodic fluctuations in population sizes. Nevertheless, the stable periodic solutions generated by the supercritical Hopf bifurcation enable species to achieve coexistence, avoiding the extinction of a single species. These findings provide a theoretical basis for ecological conservation in the context of global warming.

Author contributions. Miao Peng and Rui Zhu: Writing-original draft, writing-review and editing, methodology, investigation, software, validation; Zhengdi Zhang: Writing-review and editing, supervision. All authors have read and approved the final version of the manuscript for publication.

Acknowledgments. The authors thank anonymous referees for their valuable comments and constructive suggestions.

Conflict of interest. All authors declare that there are no conflicts of interest.

References

[1] R. Arditi and L. R. Ginzburg, *Coupling in predator-prey dynamics: Ratio-dependence*, J. Theor. Biol., 1989, 139(3), 311–326.

[2] D. Barman, V. Kumar, J. Roy and S. Alam, *Modeling wind effect and herd behavior in a predator-prey system with spatiotemporal dynamics*, Eur. Phys. J. Plus, 2022, 137(8), 950.

[3] M. Cherry and B. Barton, *Effects of wind on predator-prey interactions*, Food. Webs., 2017, 13, 92–97.

[4] W. Cresswell, *Predation in bird populations*, J. Ornithol., 2011, 152(Suppl 1), 251–263.

[5] Y. Enatsu, J. Roy and M. Banerjee, *Hunting cooperation in a prey-predator model with maturation delay*, J. Biol. Dyn., 2024, 18(1), 2332279.

[6] R. K. Goodrich, *A Riesz representation theorem*, P. Am. Math. Soc., 1970, 24(3), 629–636.

[7] B. D. Hassard, N. D. Kazarinoff and Y. H. Wan, *Theory and Applications of Hopf Bifurcation*, Cambridge University Press, Cambridge, 1981.

[8] A. R. Hayes and N. J. Huntly, *Effects of wind on the behavior and call transmission of pikas (Ochotona princeps)*, J. Mammal., 2005, 86(5), 974–981.

[9] C. S. Holling, *The functional response of predators to prey density and its role in mimicry and population regulation*, Mem. Entomol. Soc. Can., 1965, 97(S45), 5–60.

[10] K. B. Howell, *Ordinary Differential Equations, an Introduction to the Fundamentals*, CRC Press, Boca Raton, 2019.

[11] D. Jana and R. Gopal, *Complex dynamics generated by negative and positive feedback delays of a prey-predator system with prey refuge: Hopf bifurcation to chaos*, Int. J. Dyn. Control., 2017, 5(4), 1020–1034.

[12] S. Jawad, S. Roy, A. A. Thirthar and P. K. Tiwari, *Deterministic and stochastic risks assessment of excessive CO_2 emission on forest biomass under weak allee effect*, J. Appl. Math. Comput., 2025, 71(6), 9129–9156.

[13] S. Jawad, A. A. Thirthar and K. S. Nisar, *The impact of climate change on flowering plants-bees-Vespa orientalis model*, Results Control Optim., 2025, 20, 100583.

[14] E. Klimczuk, L. Halupka, B. Czyż, M. Borowiec, J. J. Nowakowski and H. Sztwiertnia, *Factors driving variation in biparental incubation behaviour in the reed warbler Acrocephalus scirpaceus*, Ardea., 2015, 103(1), 51–59.

[15] A. Kumar and B. Dubey, *Modeling the effect of fear in a prey-predator system with prey refuge and gestation delay*, Int. J. Bifurcation and Chaos, 2019, 29(14), 1950195.

[16] Y. H. Law and A. Sediqi, *Sticky substance on eggs improves predation success and substrate adhesion in newly hatched Zelus renardii (Hemiptera: Reduviidae) instars*, Ann. Entomol. Soc. Am., 2010, 103(5), 771–774.

[17] Z. Liang and X. Meng, *Stability and Hopf bifurcation of a multiple delayed predator-prey system with fear effect, prey refuge and Crowley-Martin function*, Chaos Soliton. Fract., 2023, 175, 1139555.

[18] Y. Liu and Y. Yang, *Dynamics and bifurcation analysis of a delay non-smooth Filippov Leslie-Gower prey-predator model*, Nonlin. Dyn., 2023, 111(19), 18541–18557.

[19] A. J. Lotka, *Elements of Physical Biology*, Williams and Wilkins, Baltimore, 1925.

[20] I. M. D. Maclean and R. J. Wilson, *Recent ecological responses to climate change support predictions of high extinction risk*, Proc. Natl. Acad. Sci. U. S. A., 2011, 108(30), 12337–12342.

[21] G. Mandal, L. N. Guin and S. Chakravarty, *Complex patterns in a reaction-diffusion system with fear and anti-predator responses*, Int. J. Bifurcation and Chaos, 2024, 34(12), 2450154.

[22] X. Y. Meng, H. F. Huo, X. B. Zhang and H. Xiang, *Stability and Hopf bifurcation in a three-species system with feedback delays*, Nonlin. Dyn., 2011, 64(4), 349–364.

[23] S. Pal, A. Gupta, A. K. Misra and B. Dubey, *Chaotic dynamics of a stage-structured prey-predator system with hunting cooperation and fear in presence of two discrete delays*, J. Biol. Syst., 2023, 31(02), 611–642.

[24] S. Pal, N. Pal, S. Samanta and J. Chattopadhyay, *Effect of hunting cooperation and fear in a predator-prey model*, Ecol. Complex., 2019, 39, 100770.

[25] K. Parida, B. P. Sarangi and S. Chand, *Impact of fear and anti-predator behavior on stability and chaos in multi-delayed predator-prey system*, J. Appl. Math. Comput., 2025, 71(6), 8851–8886.

[26] B. Paul, G. C. Sikdar and U. Ghosh, *Effect of fear and non-linear predator harvesting on a predator-prey system in presence of environmental variability*, Math. Comput. Simul., 2025, 227, 442–460.

[27] M. Peng, R. Lin, L. Huang and Z. D. Zhang, *Bifurcation analysis of a delayed predator-prey model with square root response functions*, J. Math., 2024, 2024(1), 8120170.

[28] M. Peng and Z. D. Zhang, *Bifurcation analysis and control of a delayed stage-structured predator-prey model with ratio-dependent Holling type III functional response*, J. Vib. Control., 2020, 26(13–14), 1232–1245.

[29] M. Peng, Z. D. Zhang, X. D. Wang and X. Y. Liu, *Hopf bifurcation analysis for a delayed predator-prey system with a prey refuge and selective harvesting*, J. Appl. Anal. Comput., 2018, 8(3), 982–997.

[30] L. Perko, *Differential Equations and Dynamical Systems*, Springer-Verlag, New York, 1991.

[31] S. Roy, D. S. AL-Jaf, A. A. Thirthar and P. K. Tiwari, *The impact of human shields in autonomous and non-autonomous prey-predator models with modified Cosner functional response*, Math. Comput. Simul., 2025, 242, 54–73.
https://doi.org/10.1016/j.matcom.2025.11.016.

[32] S. Ruan and J. Wei, *On the zeros of transcendental functions with applications to stability of delay differential equations with two delays*, Dyn. Contin. Discrete Impuls. Syst. Ser. A Math. Anal., 2003, 10, 863–874.

[33] Z. C. Shang and Y. H. Qiao, *Multiple bifurcations in a predator-prey system of modified Holling and Leslie type with double Allee effect and nonlinear harvesting*, Math. Comput. Simul., 2023, 205, 745–764.

[34] Z. H. Shen, Y. C. Xu, C. Y. Gai and J. J. Wei, *Anti-predator behavior: A mechanism to lose localized patterns for diffusive ratio-dependent predator-prey systems*, Chaos Soliton. Fract., 2026, 202, 117459.

[35] Y. L. Song and J. J. Wei, *Bifurcation analysis for Chen's system with delayed feedback and its application to control of Chaos*, Chaos Soliton. Fract., 2004, 22(1), 75–91.

[36] T. O. Svennungsen, Ø. H. Holen and O. Leimar, *Inducible defenses: Continuous reaction norms or threshold traits?*, Amer. Nat., 2011, 178(3), 397–410.

[37] A. A. Thirthar, S. Jawad and M. A. Abbasi, *The modified predator-prey model response to the effects of global warming, wind flow, fear, and hunting cooperation*, Int. J. Dyn. Control., 2025, 13, 3.
https://doi.org/10.1007/s40435-024-01504-6.

[38] A. A. Thirthar, M. Jumaah, S. Jawad, B. Kumar and M. A. Alomair, *A mathematical analysis of wind-driven bottom-up interactions in a plant-ungulate-wolf ecosystem*, Mathematics, 2026, 14(3), 418.

[39] A. A. Thirthar, B. Kumar and S. K. Verma, *Effects of predator cooperation in hunting and prey fear in a generalist predator-prey model that includes global warming phenomena*, Eur. Phys. J. Plus., 2024, 139(12), 1099.

[40] A. A. Thirthar, S. K. Nazmul, B. Mondal, M. A. Alqudah and T. Abdeljawad, *Utilizing memory effects to enhance resilience in disease-driven prey-predator systems under the influence of global warming*, J. Appl. Math. Comput., 2023, 69(6), 4617–4643.

[41] A. A. Thirthar, P. Panja, A. Khan, M. A. Alqudah and T. Abdeljawad, *An ecosystem model with memory effect considering global warming phenomena and an exponential fear function*, Fractals-Complex Geom. Patterns Scaling Nat. Soc., 2023, 31(10), 2340162.

[42] A. A. Thirthar, B. A. Sharba, S. J. Majeed, P. Panja and T. Abdeljawad, *The dynamics of prey–predator model with global warming on carrying capacity and wind flow on predation*, Nonlinear Engineering, 2026, 15(1), 20250182.

[43] J. Turner, F. Vollrath and T. Hesselberg, *Wind speed affects prey-catching behaviour in an orb web spider*, Sci. Nat., 2011, 98(12), 1063–1067.

[44] A. K. Umrao and P. K. Srivastava, *Bifurcation analysis of a predator-prey model with Allee effect and fear effect in prey and hunting cooperation in predator*, Differ. Equ. Dyn. Syst., 2025, 33(4), 1123–1149.

[45] V. Volterra, *Variations and fluctuations of the number of individuals in animal species living together*, ICES J. Mar. Sci., 1928, 3(1), 3–51.

[46] Y. Xia, X. H. Huang, F. D. Chen and L. J. Chen, *Stability and bifurcation of a predator-prey system with multiple anti-predator behaviors*, J. Biol. Syst., 2024, 32(02), 889–919.

[47] L. Zheng and Y. H. Peng, *Stability analysis of a diffusive ratio-dependent predator-prey model with nonlocal perception*, J. Nonlinear Model. Anal., 2026, 8(1), 131–144.

[48] J. Zhou, *Bifurcation analysis of a diffusive predator-prey model with ratio-dependent Holling type III functional response*, Nonlin. Dyn.,2015, 81(3), 1535–1552.

Received January 2026; Accepted May 2026; Available online June 2026.